Student thesis series INES nr 496

Analysing the vegetation condition during the 2017 and 2018 growing seasons using indices derived from Sentinel-2 data: a case study over southern Sweden

Camilla Persson

2019
Department of
Physical Geography and Ecosystem Science
Lund University
Sölvegatan 12
S-223 62 Lund
Sweden

Camilla Persson (2019)
Analysing the vegetation condition during the 2017 and 2018 growing seasons using indices derived from Sentinel-2 data: a case study over southern Sweden

Master degree thesis, 30 credits in *Geomatics*
Department of Physical Geography and Ecosystem Science, Lund University

Level: Master of Science (MSc)

Course duration: *January* 2019 until *October* 2019

Analysing the vegetation condition during the 2017 and 2018 growing seasons using indices derived from Sentinel-2 data:
a case study over southern Sweden

Camilla Persson

Master thesis, 30 credits, in *Geomatics*

Supervisor:
Abdulhakim M. Abdi
Lund University

Examiner:
Lars Eklundh
Lund University

Abstract

The summer of 2017 was climatically close to normal in southern Sweden, whereas the following summer was unusually warm and dry. These two years therefore make an interesting case study for investigating the impact of severe drought on vegetation, particularly when considering that climate change is predicted to lead to an increased frequency of drought events in the study area.

The comparison was done by calculating *vegetation indices* (VI) based on satellite imagery. The calculated indices are *Normalised Vegetation Index* (NDVI), *Enhanced Vegetation Index* (EVI) and *Normalised Difference Water Index* (NDWI) based on four Sentinel-2 images from 2017 and four images from 2018. Rain Use Efficiency (RUE) was calculated based on NDVI and EVI and a precipitation data set from PERSIANN-CCS, in an attempt to measure drought resilience. The data was extracted for different land covers and crop types to determine where the largest differences were seen in the study area.

It was found that the land cover with the smallest decreases (and some increases) in VI values between the two years was mixed forest. Both coniferous and deciduous forest had more negative changes between the two years; this suggests that the combination of tree types could increase the drought resilience. The land cover with the largest decrease was agricultural land which had decreasing values for all VI's, suggesting that this might be the least drought resilient land cover.

The break-down of the changes by crops showed that part of the decrease in VI values between 2017 and 2018 in agricultural land could be explained by a shift from winter crops to spring crops due to the late harvest in 2017. It could also be a result of the satellite imagery from the different years being taken at different dates, and capturing different stages of the growing cycle which would affect the results of cereal crops and rapeseed in particular. The largest decrease in VI values were seen in winter wheat and spring barley which indicates that these might be more drought sensitive. Both RUE and the standard deviation of RUE increased for the whole study area between the two years, which is likely a result of the large amount of precipitation amounts in 2017.

Keywords: Physical Geography, Ecosystem Analysis, Remote Sensing, Vegetation Indices, Drought, Geomatics

Abstract (Swedish)

Sommaren 2017 uppfattades av många som ovanligt blöt och kall, men var i själva verket nära det normala i södra Sverige, medan sommaren efter (2018) var ovanligt varm och torr. Dessa två år utgör därför en intressant fallstudie för att undersöka hur extrem torka påverkar vegetationen i södra Sverige. Jämförelsen är särskilt intressant eftersom klimatförändringarna bland annat förväntas leda till en ökad frekvens av torka i området.

Jämförelsen mellan de två åren gjordes genom att räkna ut *vegetations index* (VI) baserat på satellitbilder för att mäta vegetationens hälsa och vätskeinnehåll. Uträkningarna baserades på åtta bilder från Sentinel-2, fyra från 2017 och fyra från 2018. De index som användes är *Normalised Vegetation Index* (NDVI), *Enhanced Vegetation Index* (EVI) och *Normalised Difference Water Index* (NDWI). *Rain Use Efficiency* (RUE) räknades ut baserat på NDVI och EVI samt nederbördsdata från PERSIANN-CCS, i ett försök att mäta hur resistent vegetationen var mot torka. Data extraherades för olika marktäcken och grödor för att undersöka var de största skillnaderna mellan åren kunde ses.

Marktäcket med minst minskning i (och viss ökning) i vegetations index (VI) värden mellan de två åren var blandad barr- och lövskog. Både barrskog och lövskog hade större negativa skillnader än blandad skog; vilken pekar mot att kombinationen av barr- och lövskog skulle kunna öka resistensen mot torka. Marktäcket med den största minskningen i VI värden var odlad mark, där värdena var lägre för alla VI, vilket indikerar att det är det marktäcke som är mest känsligt mot torka.

Vidare undersökning av skillnaderna i VI värden för olika grödor visade att en del av de skillnader som sågs i odlad mark kan förklaras med att det odlades mer vårgrödor 2018 än 2017 på grund av den sena skörden 2017. Men skillnaderna kan också bero på att satellitbilderna är tagna vid olika tidpunkter under de två åren, och därför kan ha fångat växterna i olika utvecklingsskeden. Det här skulle framförallt kunna påverka resultaten för spannmål och raps. Den största minskningen av VI värden kunde ses i höstvete och vårkorn, vilket skulle kunna indikera att de är mer känsliga mot torka än andra grödor. Både RUE och standardavvikelsen i RUE ökade i hela studieområdet, vilket troligen beror på den stora mängden nederbörd under 2017.

Nyckelord: Naturgeografi och Ekosystemanalys, Fjärranalys, Vegetations Index, Torka, Geomatik

Table of contents

1. Introduction

The summer of 2017 was perceived by many in Sweden as wet and cold (Aftonbladet, 2017a, 2017b), but was in fact climatically close to a normal Swedish summer (SMHI, 2017). The summer of 2018 stood in stark contrast to 2017, particularly in light of the severe drought that swept across Europe and caused of loss of income to farmers in Sweden (LRF, 2018). Scania, which has large area of farmland in Sweden, was particularly affected (Länsstyrelsen, 2018).

Climate change will likely result in higher temperatures, larger amounts of precipitation in southern Sweden (Maracchi et al., 2005), and a prolonged growing season (Wiréhn, 2018). This is largely predicted to have a positive impact on vegetation in norther Europe as temperature and the length of the growing seasons both are limiting factors (Maracchi et al., 2005; Olesen et al., 2007). However, climate change will also increase the likelihood of extreme events such as heavy rainfall days and severe droughts (Trnka et al., 2011) with high losses and economic damages (Trnka et al., 2014).

The last drought to severely impact the agricultural sector in Europe was in 2003, where significant reduction in rainfall and extreme heat resulted in large losses in crop yield (Ciais et al., 2005). However, recent analysis from Buras et al. (2019) found that the 2018 drought was even more severe than 2003. Previous studies have shown that difference land covers and vegetation types respond differently to drought (Buras et al., 2019; Zaitchik et al., 2006) and that the impact of summer droughts can be particularly severe due to the combination of drought and heat stress (Mittler, 2006). Agricultural land and pasture are often affected negatively by drought earlier and to a larger extent than other land covers (Buras et al., 2019; Zaitchik et al., 2006). Particularly intense events such as the one seen during the summer of 2003 and 2018 make interesting case studies as we can see how different types of vegetation can react to, and mitigate against, extreme temperatures and lack of rainfall.

Satellite remote sensing data will be used in order to observe the differences between the 2017 and 2018, as it allows data to be collected in a consistent way, over larger areas and with higher temporal resolution than other types of remote sensing (Niemeyer, 2008). The high temporal resolution makes it possible to study changes over time, through time series analysis, and with remotely-sensed data we can more easily detect spatial variability in vegetation.

The aim of this study is to quantify the effects of the particularly severe drought of 2018 on the vegetation in southern Sweden in comparison to the relatively normal summer of 2017. The objective is to find if there are land cover or crop types that are especially vulnerable to extreme drought in this area. The study consists of two main sections; a literature study and analysis of satellite data covering the study area for the summers of 2017 and 2018. The literature study will focus on the effect of climate change on vegetation, vegetation response to drought and remote sensing of vegetation. The second part of the study will be based on analysis of gridded spatial data over the study area. Here the impact of drought on vegetation will be investigated by calculating the vegetation indices: Normalized Difference Vegetation Index (NDVI), Enhanced Vegetation Index (EVI) and Normalized Difference water Index (NDWI) for four dates for each of the growing seasons in 2017 and 2018,

based on satellite data from Sentinel-2. The values will then be extracted based on vegetation land covers from Naturvårdsverket (Ahlkrona et al., 2018) and crop data from Jordbruksverket (2018a) and compared between the two years. Rain use efficiency (RUE) will be calculated based on NDVI and EVI and precipitation data from PERSIANN-CCS (Nguyen et al., 2019) in an attempt to measure drought resilience. These values will also be extracted based on land covers and crops, to see if there are any differences.

2. Background

2.1. Climate change and vegetation

Both temperature and precipitation is expected to increase in northern Europe due to climate change (Maracchi et al., 2005). This will likely result in milder winters and longer summers in Sweden (Maracchi et al., 2005; Olesen et al., 2007). Although precipitation is projected to increase, summer droughts are also expected to become more common (Trnka et al., 2011), as is heavy rainfall days (Wiréhn, 2018) and extreme weather events (Kovats et al., 2014) which could result in losses in yield (Rötter et al., 2013).

In northern Europe crop productivity is limited by temperature and the short length of the growing season (Maracchi et al., 2005). Climate change, with higher temperatures and longer growing seasons, in combination with higher CO2 levels is largely predicted to have a positive impact on agriculture in northern Europe (Alcamo et al., 2007; Maracchi et al., 2005; Olesen et al., 2007). The winter wheat yield is expected to increase (Olesen et al., 2007), as well as onion, (Maracchi et al., 2005) sugar beets and potato, although potato yields are sensitive to large temperature increases, and yields could decrease with continued climate change (Supit et al., 2012).

However, a changing climate does of course present some challenges. Secondary effects of climate change could also affect crop health and yield. Milder winters increase the risk for plant diseases, insects, weeds and fungus in the soil, as more of these will survive the winter in a warmer climate (Kovats et al., 2014). Higher temperatures could also result in quicker maturity and lower yield especially for cereal crops such as winter wheat (Maracchi et al., 2005). Crop varieties that are better suited to longer growing seasons could be introduced to decrease the impact of increasing temperature on cereal crop yield (Olesen et al., 2012). However, increasing temperatures also present an opportunity to introduce new crop varieties and crops like maize could be farmed at a larger scale than what is currently possible (Olesen et al., 2007).

Although crop yield is generally expected to increase due to climate change, precipitation variability and drought is projected to become more common, leading to higher event-based losses and economic damages across these events (Trnka et al., 2014). Drought is more difficult to prepare for than a gradual increase in temperature and affects plants and crops more acutely. In particular, harsh droughts associated with the increase in extreme climatic events in some projections (Li et al., 2009; Spinoni et al., 2018) could be especially harmful given the difficulty in predicting drought events

(Grasso & Singh, 2011) and the difficulty in adapting to irregular fluctuations (Toreti et al., 2019). The 2018 heatwave brought substantial agricultural (LRF, 2018) and social (Åström et al., 2019) damages, and drought present a significant challenge as the world's climate alters further.

2.2. Drought and vegetation

Plants are exposed to different types of stress on a daily basis. These can include heat, low temperature, drought, frost, insects, mineral deficits, flooding, and disease (Lichtenthaler, 1996; Mittler, 2006). Drought is one of the plant stresses with the largest adverse effects (Shao et al., 2009) and the plant responses to these events are highly complex (Chaves et al., 2003). The response to a combination of different stresses is different to the response to the same stresses happening one at a time, and cannot always be predicted based on responses to singular stresses (Mittler, 2006; Rizhsky et al., 2004). The impacts on plant health have been found to be more severe in cases where droughts are combined with high heat (Mittler, 2006). Common plant responses to drought are closed stomata, decreasing photosynthesis, decreased plant productivity (Mittler, 2006; Shao et al., 2009) but different plant types have different coping mechanisms (Barnabás et al., 2008; Chaves et al., 2003). The impact on the plant will also depend on the timing, length and severity of the drought (Bartels & Souer, 2004). It is also interesting to note that there is a difference between crop yield and plant survival. Bruce et al. (2002) and Quarrie et al. (1999) both point out that a short reaction time to drought might be good for plant survival but not necessarily for crop yield.

There are three main types of coping mechanisms; escape, avoidance and tolerance (Turner, 1986). Escape strategies are when the plant will speed up the growing cycle to finish the reproductive stage before it is adversely affected by drought (Chaves et al., 2003). This is a common coping mechanism in cereal crops and relies on the plant having enough reserves stored to produce fruit (Bruce et al., 2002). Avoidance strategies are coping mechanisms where the plant will attempt to decrease the effect of drought as much as possible, by minimising water loss and maximising water uptake (Chaves et al., 2003). This is done by closing the stomata (Barnabás et al., 2008), and decreasing the leaf area through rolling leaves (Kadioglu & Terzi, 2007), adjusting the leaf angle, and shedding old leaves, and growing roots (Barnabás et al., 2008; Chaves et al., 2003). Avoidance strategies are seen in a wide range of plant types ranging from grasses (Kadioglu & Terzi, 2007), to deciduous (Varela et al., 2010) and coniferous trees (Martínez-Ferri et al., 2000). Tolerance involves the plant developing ways in which it can be more resistant to drought conditions, such as developing smaller, thicker leaves, that are better at coping with low precipitation and high temperature (Larcher, 2000). Tolerance strategies are commonly seen trees in the Mediterranean area (Larcher, 2000; Martínez-Ferri et al., 2000).

A plant can use a combination of different strategies to cope with drought (Price et al., 2002). Rice, for example, combines avoidance, tolerance and escape mechanisms; it can speed up its growing cycle associated with escape strategies, develop deeper roots associated with drought avoidance, and make osmotic adjustments associated with tolerance strategies (Price et al., 2002).

Drought resilience can also be affected by plant composition in the area. It is not yet understood how mixed forests are coping with drought compared to forests with just one kind of tree species (Pretzsch et al., 2013). But it is suggested that mixed forest stands could gain from niche complementarity and therefore be more resilient to drought (Morin et al., 2011). Similar results have been seen before by Pretzsch et al. (2013) who studied Norway spruce, sessile oak and European beech, and found that although the drought resistance of sessile oak and Norway spruce did not change between pure and mixed forests, European beech became more resilient when mixed with especially oak. Gazol and Camarero (2016) found improved resilience in forests with silver fir, scots pine and European beech. However, Merlin et al. (2015) found no improvement in drought resilience when scots pine and sessile oak were mixed.

2.3. Satellite-based spectral indices

In order to communicate and compare the severity of droughts, they need to be quantified. There are a vast amount of indices and indicators that can be used for this purpose, focusing on many different factors (AghaKouchak et al., 2015; Niemeyer, 2008; Zargar et al., 2011). Vegetation indices (VI) used for quantifying agricultural droughts often focus on vegetation health (Hazaymeh & Hassan, 2017), soil moisture (AghaKouchak et al., 2015) and evaporation (Glenn et al., 2010).

Historically drought indices have been based on *in situ* measurements of precipitation, soil moisture and evaporation (AghaKouchak et al., 2015). With *in situ* measurements the results will be very accurate at a local scale, and you can measure the factors that directly affect the vegetation. However, it is difficult to cover larger areas, and creating spatial data relies on interpolating between the measuring stations, which has some limitations (Du et al., 2013; Rhee et al., 2010).

Satellite imagery allows data to be collected in a consistent way, over larger areas and with higher temporal resolution than other types of remote sensing (Niemeyer, 2008). The high temporal resolution makes it possible to study changes over time, through time series analysis, and with remotely-sensed data we can more easily detect spatial variability. However, remote sensing data also has its limitations. There is no spectral wavelength that can in itself directly tell us about soil moisture or evaporation (Glenn et al., 2010). Therefore, these parameters must be estimated by combining different spectra and empirically testing them. In this way, different indices can be used to quantify drought impacts using remotely-sensed data.

It is also important to acknowledge that there is a difference between vegetation status and vegetation water content. Using vegetation status indices as a drought index assumes that the vegetation health and the greenness of plants are correlated to the moisture content of the plant (Ceccato et al., 2001). This is mostly true, and drought is one of the environmental stresses with the most severe negative impacts on crops (Shao et al., 2009) but many other factors can affect the greenness and vegetation health, such as the plant stressors mentioned before (Mittler, 2006). In studying drought it could therefore be useful to look at indices for both vegetation status and vegetation water content (Gao, 1996) or combine different types of indices (Hazaymeh & Hassan, 2017).

As noted before different types of vegetation, plants and ecosystems have different responses to drought. Previous studies have therefore used remotely sensed images together with land cover and climate data sets to find how the responses vary. Buras et al. (2019) compared the impacts of drought on different ecosystems during the droughts in 2003 and 2018. They found that the drought in 2018 was more severe than the drought in 2003, but also that forested land covers were impacted less than grassland and agricultural land. A similar study by Zaitchik et al. (2006) also came to the same conclusion. Both of these studies used vegetation and land cover data of relatively low resolution and used data which grouped agricultural land, pastures and grassland together as a class (Buras et al., 2019; Zaitchik et al., 2006). This could be misleading since the crops grown at a certain location can vary, and the choice of crop at a particular location can depend on the weather the previous year (Holmblad et al., 2019), and what has been growing in that location before (Jordbruksverket, 2018b). Incorporating crop data could further improve the results.

3. Method

3.1. Study area

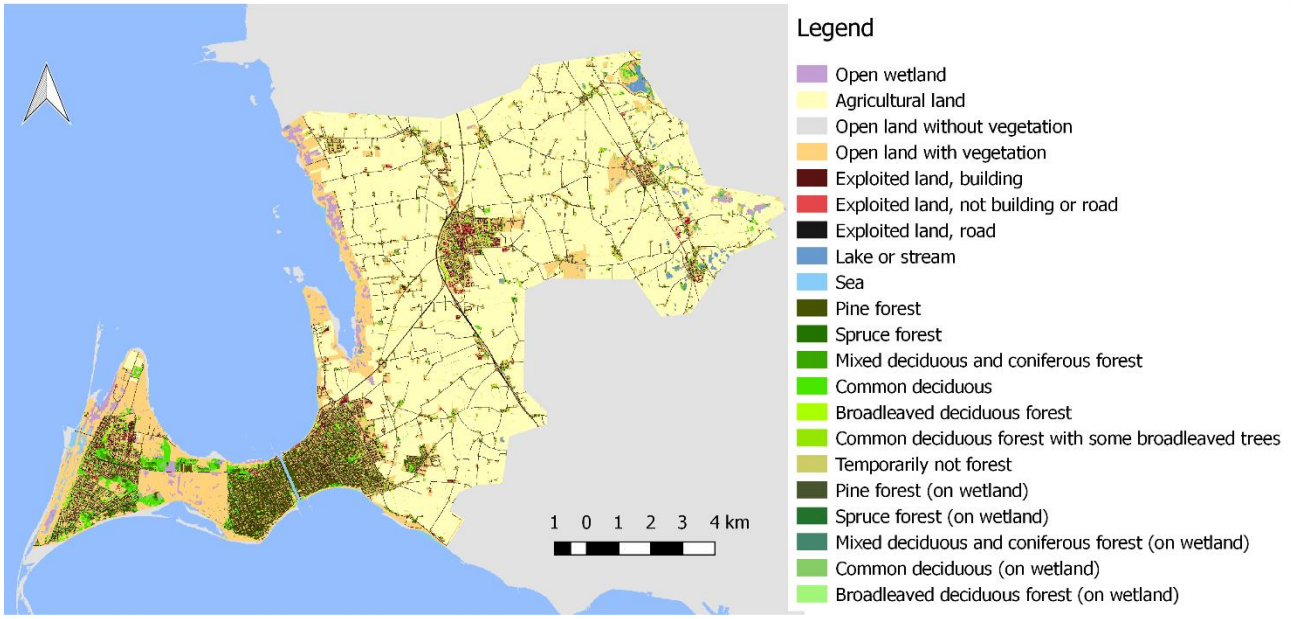

Figure 1. The study area and its land cover based on data from Naturvårdsverket (Ahlkrona et al., 2018).

The study area is Vellinge municipality located at the southwestern tip of Sweden, in the county of Scania (Figure 1). Scania is known for its relatively mild climate and has the mildest winters and the longest summers in Sweden (SMHI, 2016). The mean temperatures during the winter months are about 0°c and the mean temperature over the summer months is about 17°C (SMHI, 2016). The area is relatively flat, and the soil is arable. This combined with the mild climate makes Scania a large producer of agricultural products. Vellinge was chosen as a study area both because of the large areas of agricultural lands, but also because it had more cloud free satellite images than other areas during the growing seasons of 2017 and 2018. The majority of the study area is used for crops, but there are also some smaller built up areas, and areas of forest, wetlands, and coastal vegetation.

3.2. Data

The main datasets used to this project can be see seen in Table 1.

Table 1. The resolution, dates and references for the main datasets used in this study

Datasets	Resolution	Dates	Reference
Sentinel-2	10 m	2017 (30/4, 27/5, 19/6, 25/8) 2018 (02/5, 30/5, 04/7, 23/8)	Gatti et al. (2015)
Crop data	10 m	2017 and 2018	Jordbruksverket (2018a)
Land cover data	10 m	2018	Ahlkrona et al. (2018)
Precipitation	Originally 0.04° resampled to 10m	Monthly 2008-2018	Nguyen et al. (2019)
Precipitation	Measuring station	Monthly 1980-2018	SMHI (2019a)
Temperature	Measuring station	Monthly 1980-2018	SMHI (2019b)

3.2.1. Sentinel-2

The data analysis part of the project will primarily be based on raster data from the Sentinel-2 Multispectral Instrument. Eight Sentinel-2 scenes were used, with four each covering the 2017 and 2018 growing seasons, respectively. The Sentinel-2 data were downloaded from the Copernicus Open Access Hub in L2A processing format, which means that they are atmospherically-corrected surface reflectance measurements. All the satellite data were from Sentinel-2A except for May 30th, 2018 which was from Sentinel-2B. Sentinel-2 has 13 bands and a number of R, NIR and SWIR bands that are particularly useful for monitoring vegetation (Table 2) (Suhet, 2015).

Table 2. Details about Sentinel-2 bands with a resolution of 10-20m adapted from Suhet (2015). Bands with a coarser resolution are not shown.

	Band number	Central wavelength (nm)	Bandwidth (nm)	Resolution (m)
Blue	2	490	65	10
Green	3	560	35	
Red	4	665	30	
Near infrared	8	842	115	
Vegetation red edge (1)	5	705	15	20
Vegetation red edge (2)	6	740	20	
Vegetation red edge (3)	7	783	20	
Narrow NIR	8a	865	20	
SWIR (1)	11	1610	90	
SWIR (2)	12	2190	180	

There is a difference in spatial resolution between some of the bands used in this study. For example, the R and NIR bands are both at a 10-meter resolution whereas two of the SWIR bands (11 and 12) have a resolution of 20 meters. These bands have been resampled so that they have the same resolution and spatial extent as the 10-meter bands.

In Figure 2 we can see the distribution of Sentinel-2 images over the growing season. The first, second and fourth image of each year are taken at roughly the same dates each year, however the third date differs between the years as it was difficult to find cloud free images of the study area between July and August in 2017. This also means that there is a large gap between the third and fourth image in 2017.

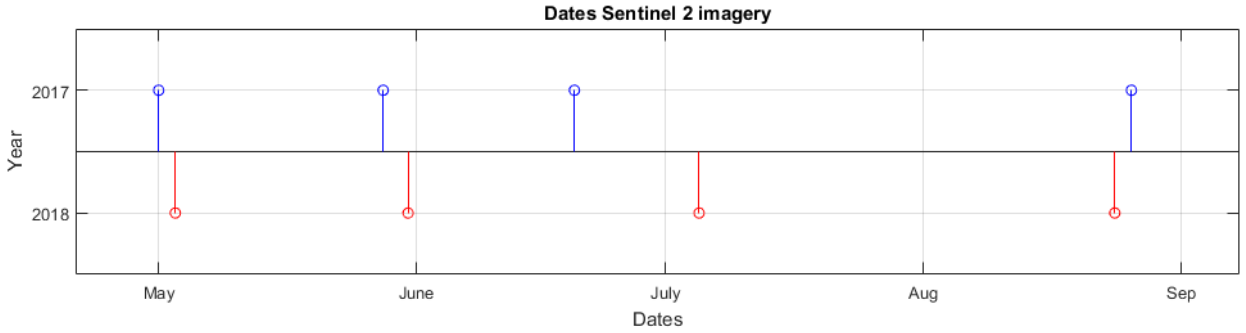

Figure 2. The dates of the Sentinel-2 images used in this study for 2017 and 2018.

3.2.2. Land cover data

The land cover data comes from Naturvårdsverket and is based on remotely sensed data from both Sentinel-2 and light detection and ranging (LIDAR) data that has been classified into land cover types (Ahlkrona et al., 2018). It is assumed that the spatial distribution of land cover has not changed much between the years, and therefore only land cover data from 2018 will be used. The areas of all land cover types in the study area can be seen in Appendix A, Figure A1. There are many land cover types in the area, and many of them are not vegetation types, or cover very small areas.

Table 3. The areas of the vegetation land covers used in this study in percentages of the whole study area and ha 2018 based on the land cover data from Naturvårdsverket (Ahlkrona et al., 2018).

	Area 2018 (ha)	**Area 2018 (%)**
Open wetland	242	2
Agricultural land	8673	61
Open vegetation	2797	20
Coniferous forest	416	3
Mixed forest	87	1
Deciduous forest	570	4

For the analysis in this project, all non-vegetated categories such as roads, sea, and buildings were removed, and the forest categories were grouped into broad forest classes; coniferous forest, mixed forest and deciduous forest. The spatial distribution of all land covers can be seen in Figure 1, and Table 3 shows the areas of the grouped vegetation types used for this project.

3.2.3. Crop data

The crop data was requested from Jordbruksverket (2018a) and are based on a crop census (Jordbruksverket, 2019a). These data are very important to consider when comparing year to year vegetation/drought indices, as crops are often rotated and not farmed in the same place every year (Jordbruksverket, 2018a). In total there are 44 different crops being farmed in the study area over these two years. All crops farmed in in the study area during 2017 and 2018 can be seen in Appendix A, Figure A2. This is a large number of categories to compare and analyse. Therefore, only the crops that were cultivated over the largest area in both years were chosen. However, before this was done four different types of pasture were grouped together ("*Slåtter och betesvall på åkermark med en vallgröda som ej är godkänd för miljöersättning*", "*Slåtter och betesvall på åker*", "*Slåtteräng (ej åker)*" and "*Betesmark (ej åker)*"), as they had very similar spectral values and properties.

Table 4. The areas of the six most common crops in percentage cropland covered and ha for 2017 and 2018 based on the crop data from Jordbruksverket (2018a)

	Area 2017 (ha)	Area 2018 (ha)	Area 2017 (%)	Area 2018 (%)
Wheat (winter)	2758	2386	29	25
Barley (spring)	1572	2113	16	22
Pasture	1447	1419	16	15
Rapeseed (winter)	1393	1019	15	11
Sugar beet	1088	1233	11	13
Vegetables	423	449	4	5

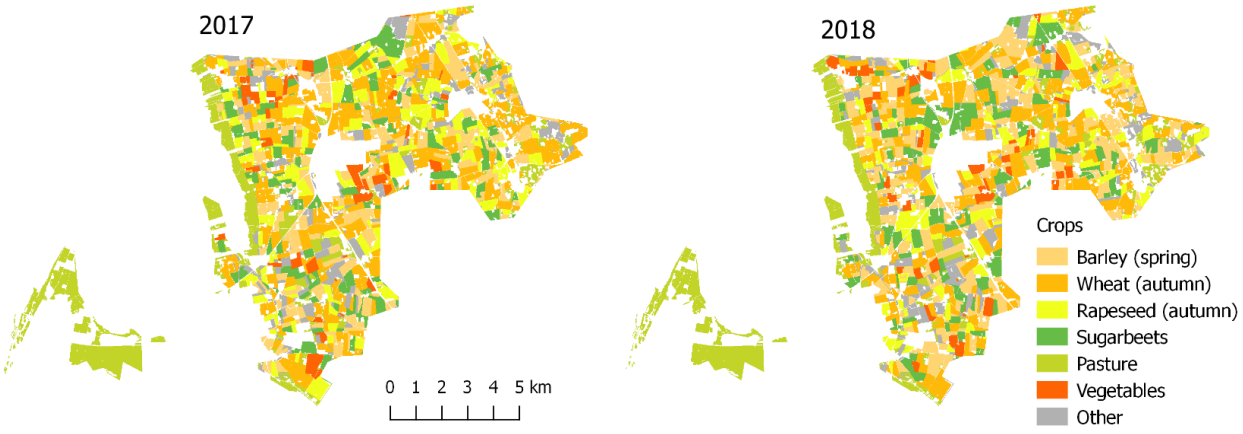

Figure 3. The spatial distribution of the six most common crops farmed in the study area in 2017 and 2018 based on the data from Jordbruksverket (2018a)

Then the selection of crops was done by calculating the percentage of the areas for each crop in each year. The crops were then sorted based on the percentage of the agricultural area each crop covered, and the crops that covered roughly 90% of the area were chosen. This resulted in six different crops, and the areas in percentages and hectares are presented in Table 4 and their spatial distribution is

shown in Figure 3. The six most common crops were the same for both years although their areal coverage varied slightly. The wheat and rapeseed varieties discussed here are planted in the autumn/winter, and the barley and sugar beet are spring crops. These crops will be referred to as just wheat, rapeseed, barley and sugar beet. There is a shift from winter crops to spring crops between 2017 and 2018 because of the late harvest in 2017 (Holmblad et al., 2019). Pasture is not farmed the same way as other crops, but will be included here since it covers a large part of the study area and therefore interesting to the results, but also since it is included in the crop data Jordbruksverket (2018a).

3.2.4. Precipitation data

In this project two types of precipitation data are used. A time series dataset based on *in situ* measurements and gridded dataset for the whole study area. The time series data from SMHI (2019a) has monthly temporal resolution and allows us to get reliable continuous data at one point in the study area. The data was collected from SMHI open data portal, and comes from a measuring station in Falsterbo, at the very southwestern corner of the study area. This measuring station was chosen as it is the only active measuring station in the area that can provide data for 2017 and 2018. Data from the years 1980-2018 were used in this study.

The gridded rainfall comes from a dataset called PERSIANN-CCS which is based on machine learning and classifying clouds based on temperature, geometry and texture (Nguyen et al., 2019). This dataset also has a monthly temporal resolution. The original projection of this data is WGS84 and it has a resolution of 0.04°. This data was re-projected, resampled and cropped to the same resolution as the other datasets (10-m) using a nearest neighbour resampling method.

3.2.5. Temperature data

Temperature time series data based on *in situ* measurements was also used. The temperature data (SMHI, 2019b) comes from the same measurement station (Falsterbo) as the precipitation data. It has a monthly temporal resolution and measurements from 1980 until 2018 were used in this study. This data was used together with the precipitation data from the same source to put the other datasets in a climate perspective since this precipitation and temperature time series data goes further back than the gridded data sets.

3.3. Calculation of vegetation indices

In this study two greenness related indices and one vegetation water content index will be used to give a better picture of the vegetation response to the two years. These indices are described in the following sections.

3.3.1. Normalized Difference Vegetation Index (NDVI)

Vegetation absorbs large amounts of radiation in the red spectrum, and less in the near infrared band (Zargar et al., 2011). The larger the normalized difference, the healthier the vegetation. NDVI (Rouse et al., 1974; Rouse et al., 1973) uses the difference in reflection in the near infrared (NIR, 842 nm) and red (R, 665 nm) bands to quantify vegetation health (Equation 1).

$$NDVI = \frac{NIR-R}{NIR+R} \qquad \textit{Equation 1}$$

It has been shown that NDVI has a high correlation with green biomass (Tucker et al., 1985). NDVI is commonly used to observe vegetation health as it is relatively easy to calculate and it has also been used to estimate the severity of droughts (AghaKouchak et al., 2015; Niemeyer, 2008). Li et al. (2002) found that there is a relationship between rainfall and NDVI but that the strength of the relationship varies spatially. The variation could be affected by annual rainfall, vegetation type and irrigation (Li et al., 2002) but the relationship is also influenced by soil type (Nicholson & Farrar, 1994) and topography (Chamaille-Jammes et al., 2007).

3.3.2. Normalized Difference Water Index (NDWI)

NDWI (Gao, 1996) was developed to better measure the water content in vegetation and uses the NIR and the shortwave infrared (SWIR, 1610 nm) bands. Many versions of this index have been developed with slight differences in the wavelengths used and with different names (Ji et al., 2011) The formula for NDWI is provided in Equation 2.

$$NDWI = \frac{NIR-SWIR}{NIR+SWIR} \qquad \textit{Equation 2}$$

Whereas in NDVI the bands R and NIR have very different absorbance for vegetation, the difference in absorption in the two bands used for NDWI is relatively small. Liquid water does not absorb much in the NIR spectrum, and it only absorbs a small amount of radiation in the SWIR band (Gao, 1996). There is also less atmospheric interference in these bands making it less sensitive to atmospheric pollution than NDVI (Gao, 1996). Gu et al. (2007) found that the NDWI responded quicker and was more sensitive to drought than NDVI.

3.3.3. Enhanced Vegetation Index (EVI)

While both NDVI and NDWI are affected by soil background (Gao, 1996), EVI was developed to be less sensitive to both soil background and atmospheric disturbances (Jiang et al., 2008). Boegh et al. (2002) studied an agricultural area in Denmark, using NDVI and EVI and found EVI to have a higher correlation with leaf area index. EVI has a higher sensitivity than NDVI for dense vegetation and high leaf biomass making it possible to observe spatial differences in high biomass regions in greater detail than what is possible with NDVI (Jiang et al., 2008; Mondal, 2011). It utilises the R, NIR and blue (B) bands where the B band is used to correct for atmospheric scattering. The formula for EVI can be seen in Equation 3.

$$EVI = \frac{2.5*(NIR-R)}{NIR+6*R-7.5*B+1} \qquad \textit{Equation 3}$$

3.3.4. Rain-use Efficiency (RUE)

RUE is the ratio between vegetation productivity and rainfall (Equation 4),

$$RUE = \frac{Productivity}{Rainfall} \qquad \textit{Equation 4}$$

RUE is a measure of the sensitivity of aboveground net primary productivity (ANPP) to variations in rainfall (Huxman et al., 2004) and drought (Ponce-Campos et al., 2013). It was originally used by LeHouerou (1984) and is often used as an indicator of land degradation and desertification in semiarid areas where relationship between vegetation productivity and precipitation is generally quite stable (Bai et al., 2008; Higginbottom & Symeonakis, 2014). Although NDVI is most commonly used as a proxy for ANPP (Bai et al., 2008; Fensholt & Rasmussen, 2011), RUE has also been calculated using EVI as proxy for ANPP in previous studies (Ponce-Campos et al., 2013; Zhao et al., 2018).

2.1. Data analysis

The means of the vegetation indices over the growing season were calculated for each pixel in the gridded data and used as measure of each season's productivity (i.e. ANPP). The mean VI for the whole season was calculated by calculating the area under the line created by the VI values from the four dates each season for each pixel (Figure 4), and then dividing this by the number of days between the first and last image each year. It is calculated this way to better account for the difference in dates of the images for both years. RUE was calculated in a similar way by calculating the mean precipitation per day between April and August based on the monthly gridded precipitation data set and dividing the mean daily NDVI and EVI by the mean daily precipitation.

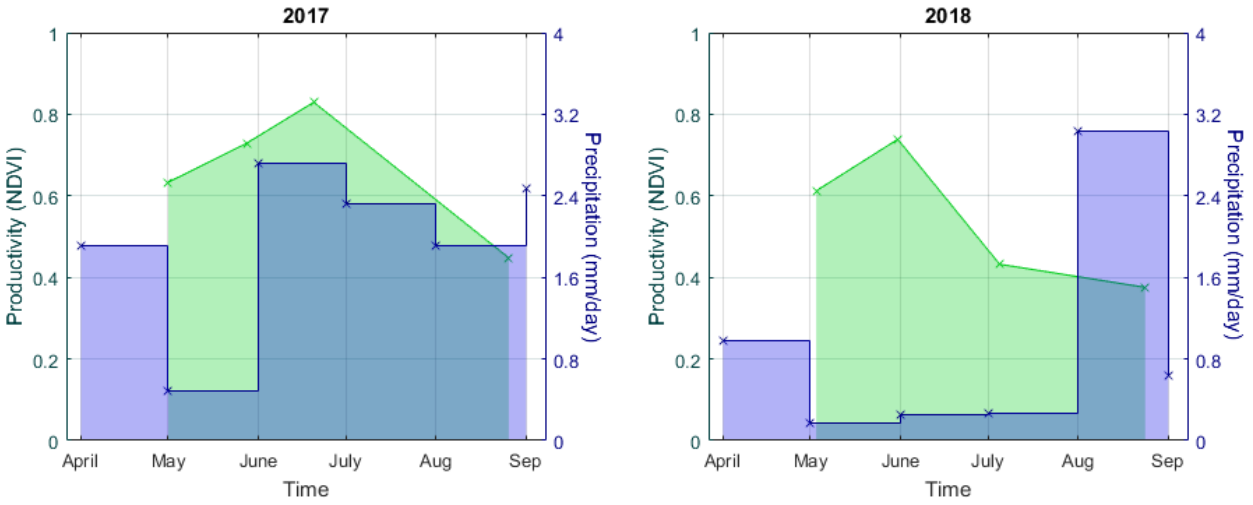

Figure 4. A conceptual model visualizing a VI and the area used to calculate the mean over the growing season (in green) and the precipitation data (in blue) used together with the VI mean to calculate RUE.

These values were extracted for the regrouped land covers and crops. The data was then visualised and presented in maps, and boxplots to show the distribution both spatially and in terms of values. The changes in means and standard deviation (SD) of NDVI, EVI, NDWI, RUE_{NDVI} and RUE_{EVI} were calculated for the whole area and for each land cover and crop category. All tables in the main

text show relative changes which are calculated as in Equation 5, where *x* is either the median or the SD.

$$Relative\ change = \frac{x_{2018} - x_{2017}}{|x_{2017}|} \qquad \textit{Equation 5}$$

Statistical tests were used to test differences in medians and distribution of values between the two years. A two-sample Wilcoxon signed rank test (Wilcoxon et al., 1970) was used to test if there is a difference in medians between the values of 2017 and 2018. For changes in distribution of values a median-adjusted two-sample Ansari-Bradley test was used (Ansari & Bradley, 1960). These tests were chosen because the distribution of the VI values for most crop and land cover categories are not normally distributed, and non-parametric hypothesis tests are therefore the appropriate choice (McCrum-Gardner, 2008). A number of different tests were used to determine if the samples were normally distributed, including a one-sample Kolmogorov-Smirnov test (Massey Jr, 1951), an Anderson-Darling test (Anderson & Darling, 1954), and the null hypothesis of normal distribution was rejected for all land cover and crop categories at a significance level of 0.05. The Wilcoxon signed rank test and Ansari-Bradley test were tested for all land cover and crop categories at a significance level of 0.05.

4. Results

4.1. Drought severity

4.1.1. Climate

The average monthly temperature and precipitation for 2017 and 2018, and a reference period 1980-2010 are shown in Figure 5. Here the temperatures in 2017 follow the reference period quite closely for most of the year whereas the temperatures in 2018 are higher during the growing season. In terms of precipitation 2017 is generally wetter than the reference period for most months, whereas 2018 is dryer.

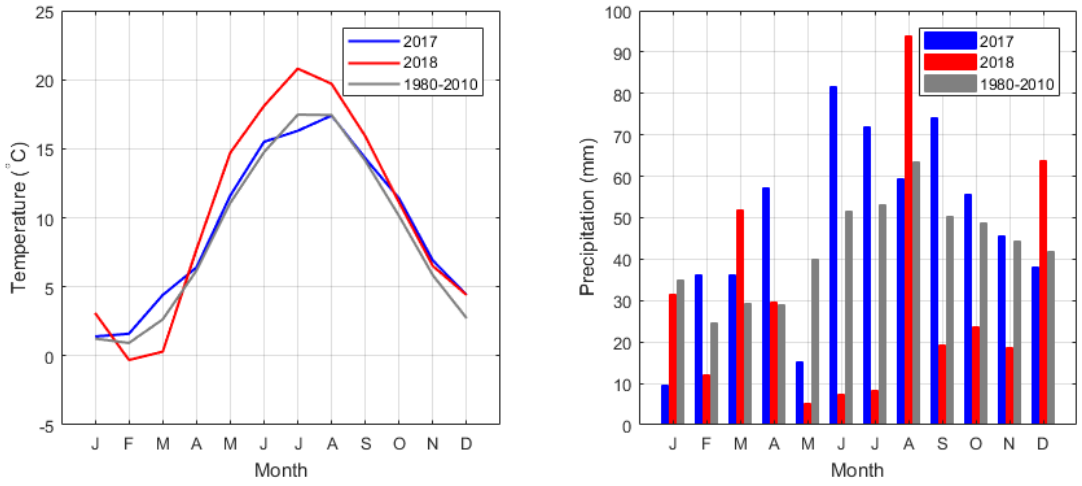

Figure 5. The average temperature and precipitation in 2017, 2018 and a reference period 1980-2010.

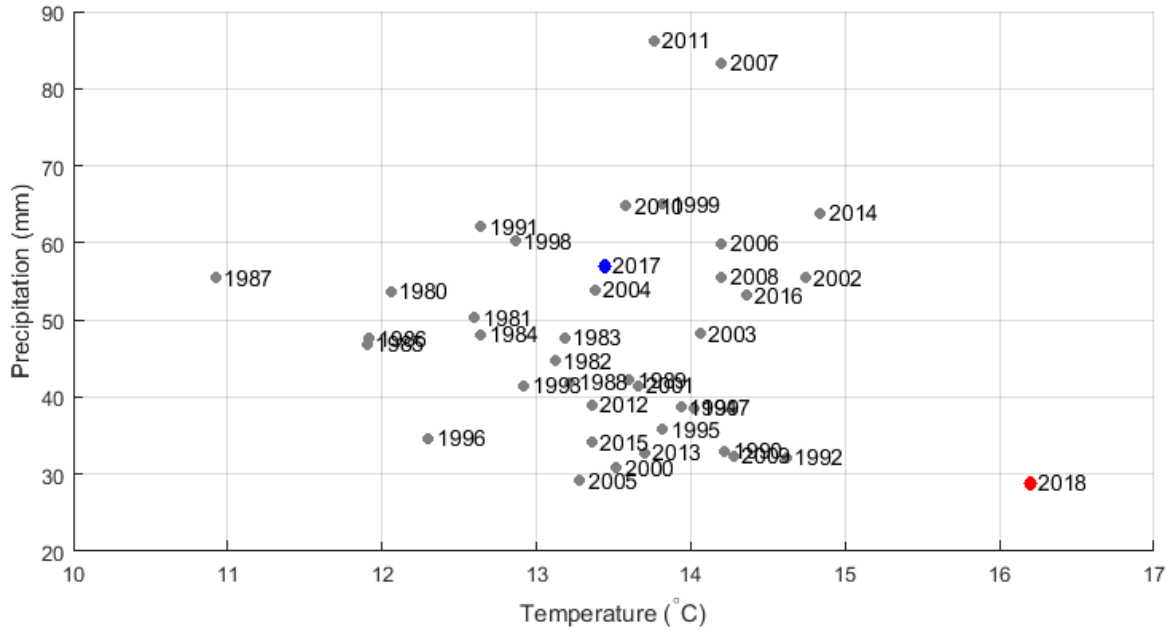

Figure 6. The average monthly temperature and precipitation per year during April-August 1980-2018.

The yearly mean temperatures and precipitation in 2018 stand out by being both one of the warmest years in the study area, but also one of the driest since 1980 (Figure 6).

4.2. Vegetation response

4.2.1. Whole study area

The VI values are higher in 2017 than in 2018 for most dates (Figure 7). The values are quite similar in 2017 and 2018 for first, second and fourth image each year and the largest differences can be seen in between mid-June and mid-July. The indices capturing vegetation health (NDVI and EVI) show similar patterns to each other but differ slightly from NDWI which has a smaller decrease between the second and third image in 2018 than NDVI and EVI.

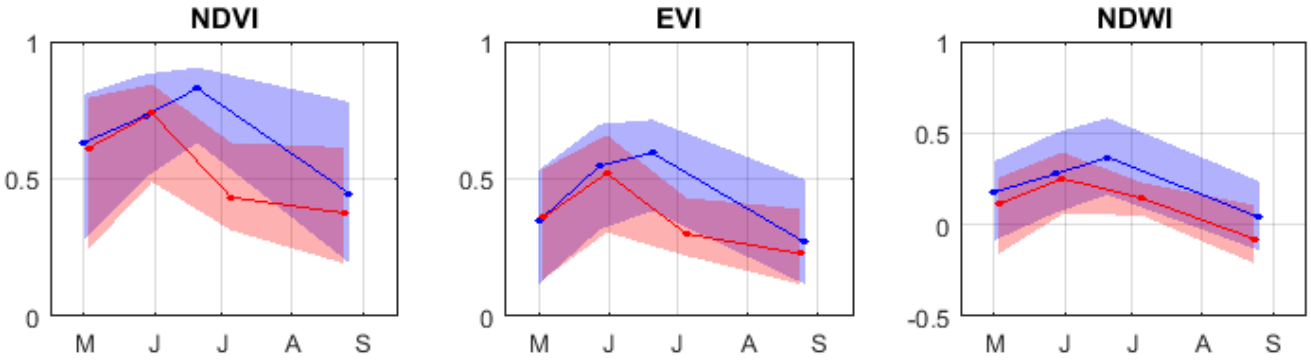

Figure 7. The medians presented as lines, and the 25th-75th percentiles presented as shaded areas of the NDVI, EVI and NDWI during the growing season for the study area for 2017(blue) and 2018 (red)

Figure 8 shows the difference in averages between 2017 and 2018 in NDVI, EVI and NDWI. The change between the two years is generally negative for most of the area, but there are small areas where increases occur. It also seems like the areas with the negative and positive change between the two years are the same for different VI's. The relative differences are larger for NDWI than for NDVI and EVI.

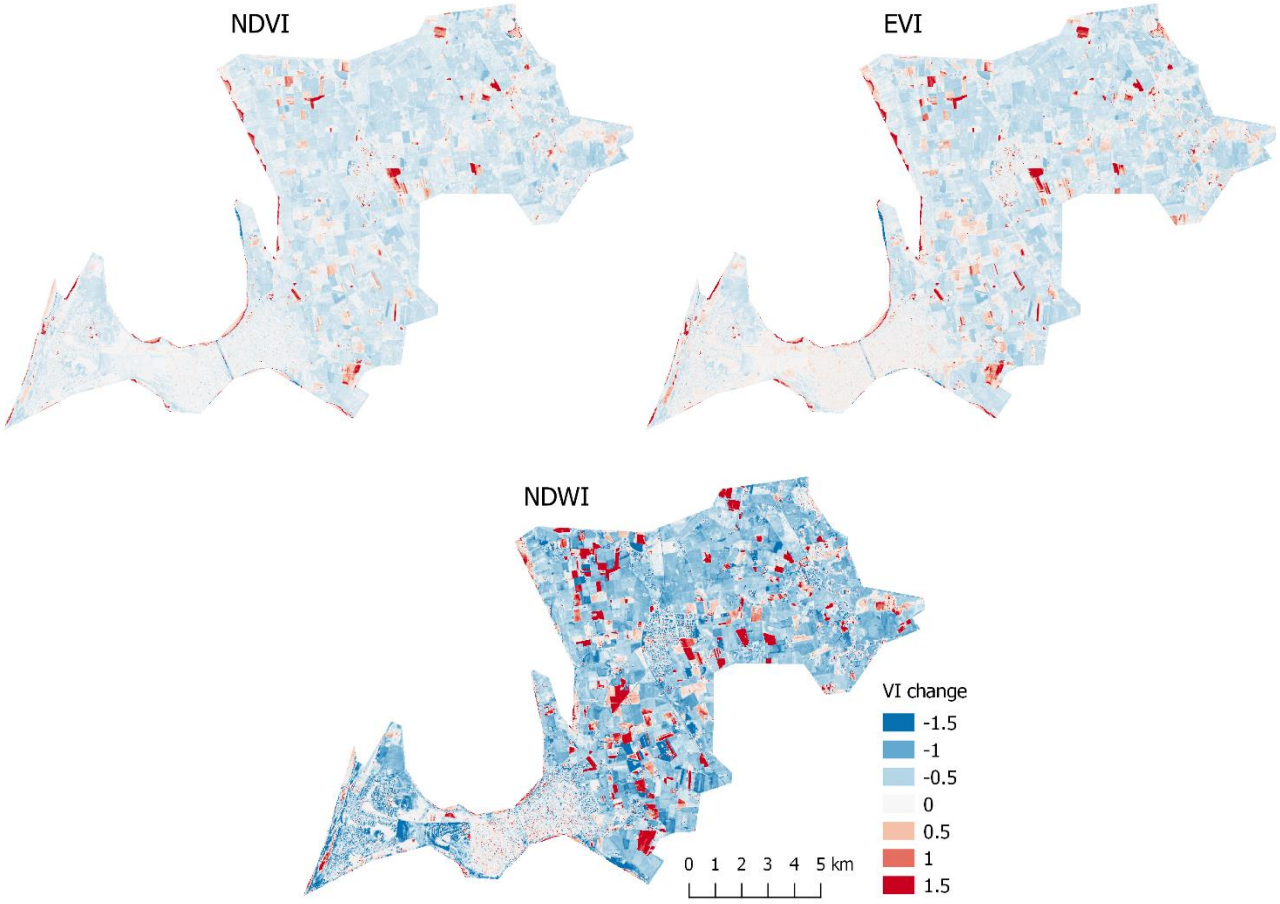

Figure 8. The relative change in mean NDVI, EVI and NDWI between the growing seasons of 2017 and 2018.

Table 5 is summarising the changes in NDVI, EVI, NDWI, Precipitation, RUE_{NDVI}, RUE_{EVI} for the whole study area. The median VI values seem to have decreased between 2017 and 2018, with the largest decrease seen in NDWI. There is also a decrease in precipitation (by almost 50%) and a large increase in mean RUE_{NDVI} and RUE_{EVI} between the two years. The standard deviation is showing similar patterns; there has been a decrease in standard deviation for all VI's, but the largest decrease is seen in NDWI. There is also a decrease in standard deviation for precipitation, and a large increase in standard deviation for RUE.

Table 5. The relative difference in medians and standard deviation in variables between the growing seasons in 2017 and 2018 for the whole study area NDVI, EVI, NDWI, Precipitation, RUE_{NDVI} and RUE_{EVI}. All differences are statistically significant at a 0.05 significance level. Negative changes are shaded. Values for each year and actual changes can be found Appendix B (Table B1 & B2).

	NDVI	EVI	NDWI	Prec	RUE_{NDVI}	RUE_{EVI}
Δ median	-0,248	-0,264	-0,594	-0,492	0,993	0,993
Δ SD	-0,099	-0,178	-0,187	-0,061	2,312	2,086

4.2.2. By land cover

Figure 9 shows the medians and the 25^{th}-75^{th} percentile of the vegetation indices per land cover over the growing seasons 2017 and 2018. Different land cover classes appear to have different growing patterns. Agricultural land for example, has increasing values in the beginning of the season, and then a decrease at the end of season, whereas the other land covers have more similar VI values throughout the season. For agricultural land the VI values are lower in 2018 at the very beginning of the season and around July, the values in June and late August are quite similar. The temporal growing pattern for wetland and open vegetation are similar to each other, with a slight increase in VI values in spring, and then quite stable values during the rest of the season in 2017, but in 2018 there is a decrease in VI values over time after the two first images. The forest land cover types display much more stable VI values over time, especially the coniferous forest. For the mixed and the deciduous forest, the values are a bit lower at the beginning the season both years, but increase and remain quite stable for the rest of the season in 2017. In 2018 there is a decrease in VI towards the end of the season. The decrease is larger in deciduous forest than in mixed and coniferous forest.

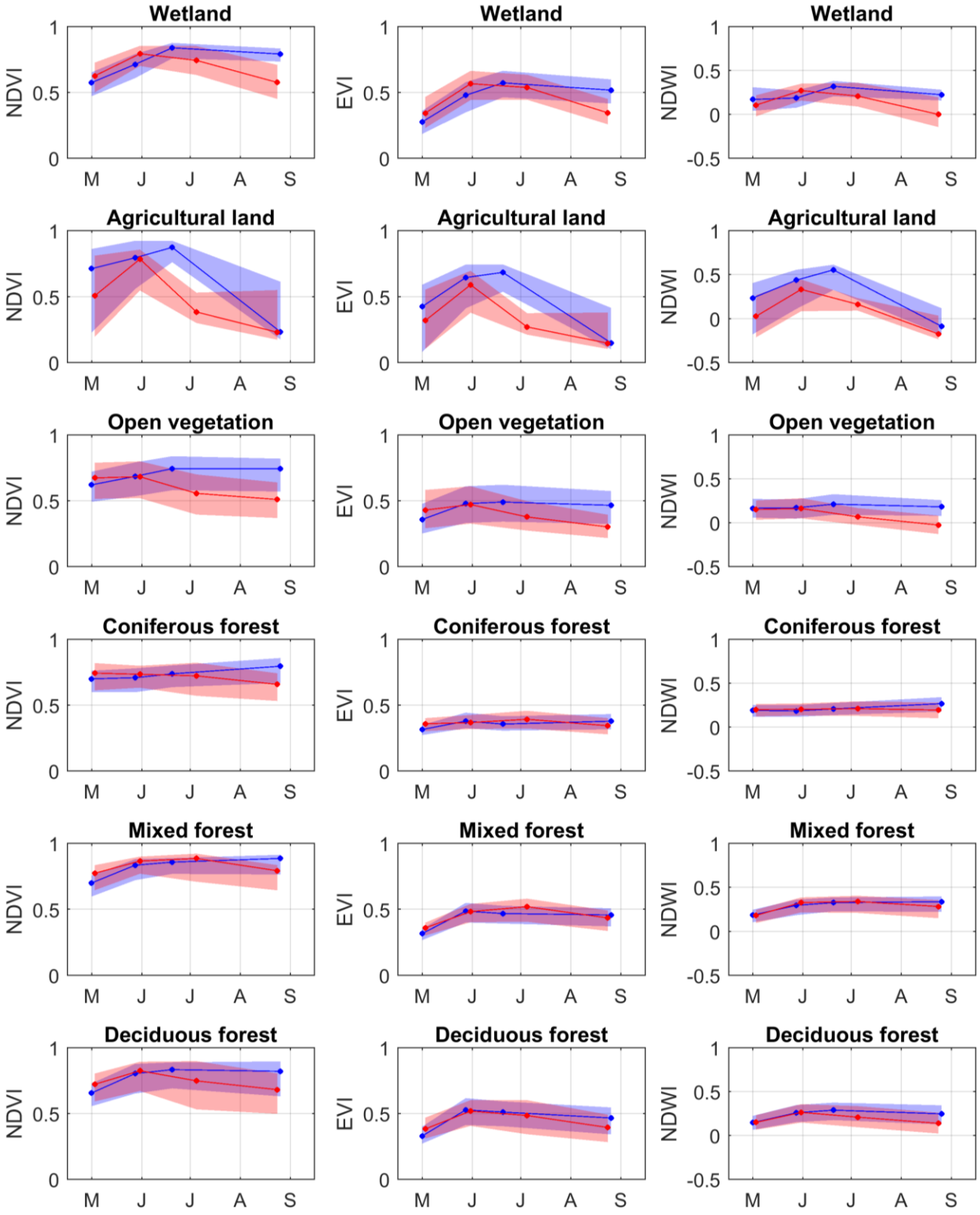

Figure 9. The medians of each image for each land cover class presented as lines, and the 25th-75th percentiles presented as shaded areas of the NDVI, EVI and NDWI during the growing season for the study area for 2017(blue) and 2018 (red).

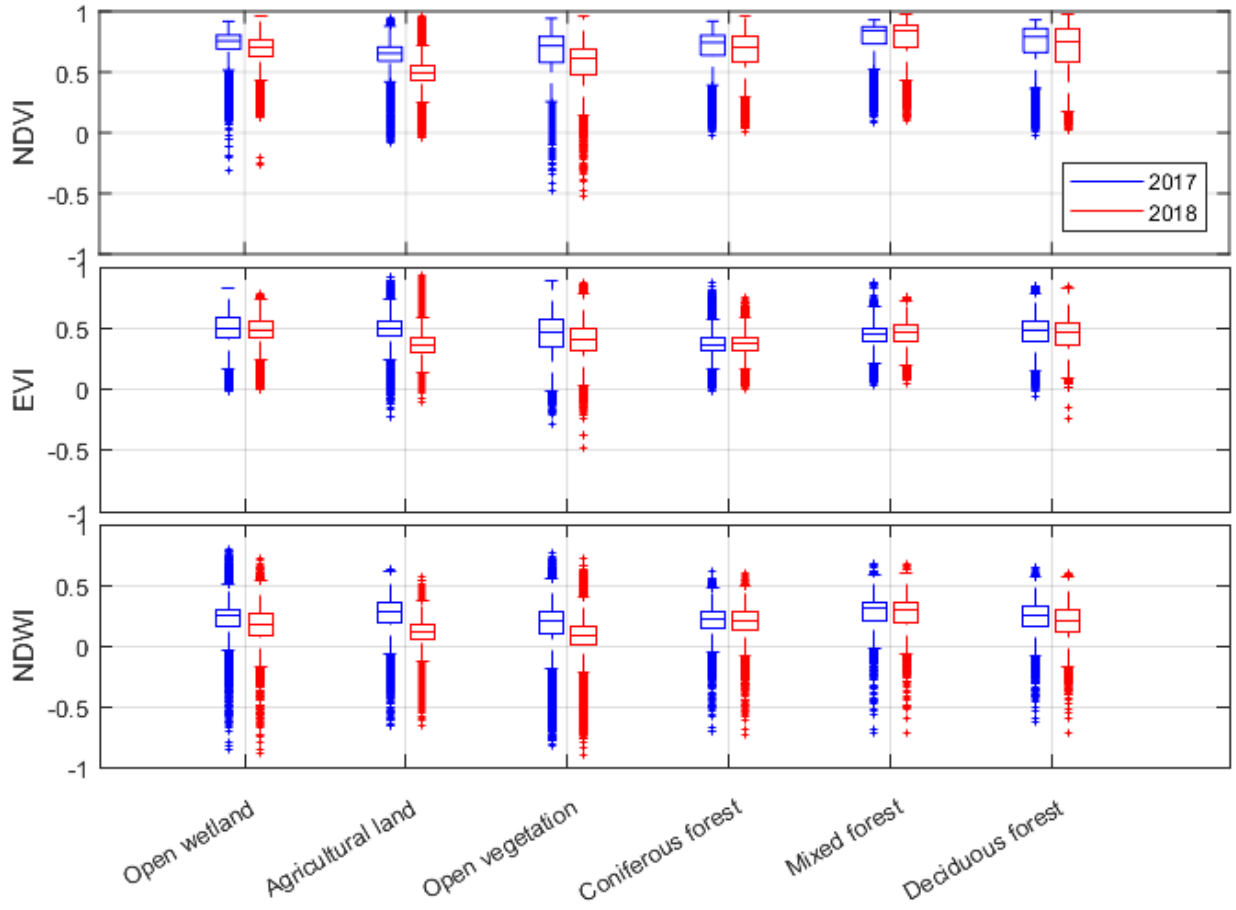

Figure 10. Boxplot showing the distribution of seasonal means of NDVI, EVI and NDWI for each land cover class during the growing seasons in 2017 and 2018. The box shows the 25th to the 75th percentile, and the line in the box represents the median. The whiskers include values up to +/-2.7σ.

The distribution of the mean VI values for the aggregated land cover types is showed in Figure 10. The values in 2018 are generally lower for all VI's. The largest negative differences are found in agricultural land, and the smallest changes are seen in mixed and coniferous forest. The changes in medians for the land cover types between the 2017 and 2018 are displayed in Table 6. The change in medians between the two years is negative for almost all land covers classes and VI's apart from and NDVI and EVI in mixed forest and EVI in coniferous forest which have a positive change between the two years. The largest decreases for all VI's are seen in agricultural land and open vegetation.

*Table 6. Relative change in median NDVI, EVI and NDWI for each land cover type between 2017 and 2018. The **bold** values are **not** statistically significant using a two sample Wilcoxon signed rank test at a 0.05 level. Negative changes are shaded. Values for each year and actual changes can be found Appendix B (Table B3 & B4).*

	Open wetland	Agricultural land	Open vegetation	Coniferous forest	Mixed forest	Deciduous forest
Δ NDVI	-0,079	-0,261	-0,168	-0,046	**0,005**	-0,062
Δ EVI	-0,026	-0,300	-0,134	0,021	0,044	-0,034
Δ NDWI	-0,363	-0,635	-0,627	-0,081	-0,012	-0,231

Table 7. Relative change in standard deviation of NDVI, EVI and NDWI for each land cover type between 2017 and 2018. All changes are statistically significant using a two sample Ansari-Bradley test at a 0.05 level. Negative changes are shaded. Values for each year and actual changes can be found Appendix B (Table B5 & B6).

	Open wetland	Agricultural land	Open vegetation	Coniferous forest	Mixed forest	Deciduous forest
Δ NDVI	0,060	-0,152	-0,070	0,083	0,128	0,130
Δ EVI	-0,135	-0,195	-0,161	-0,037	0,052	0,043
Δ NDWI	0,039	-0,278	-0,105	0,060	0,062	0,070

Table 7 shows the difference in SD for the land cover types between the two years. Interestingly, there has been an increase in SD for most forest land cover classes apart from EVI in coniferous forest and a decrease in SD for agricultural land and open vegetation. The change in SD for wetland is a bit more mixed; there is an increase in in NDVI and NDWI and a decrease in EVI.

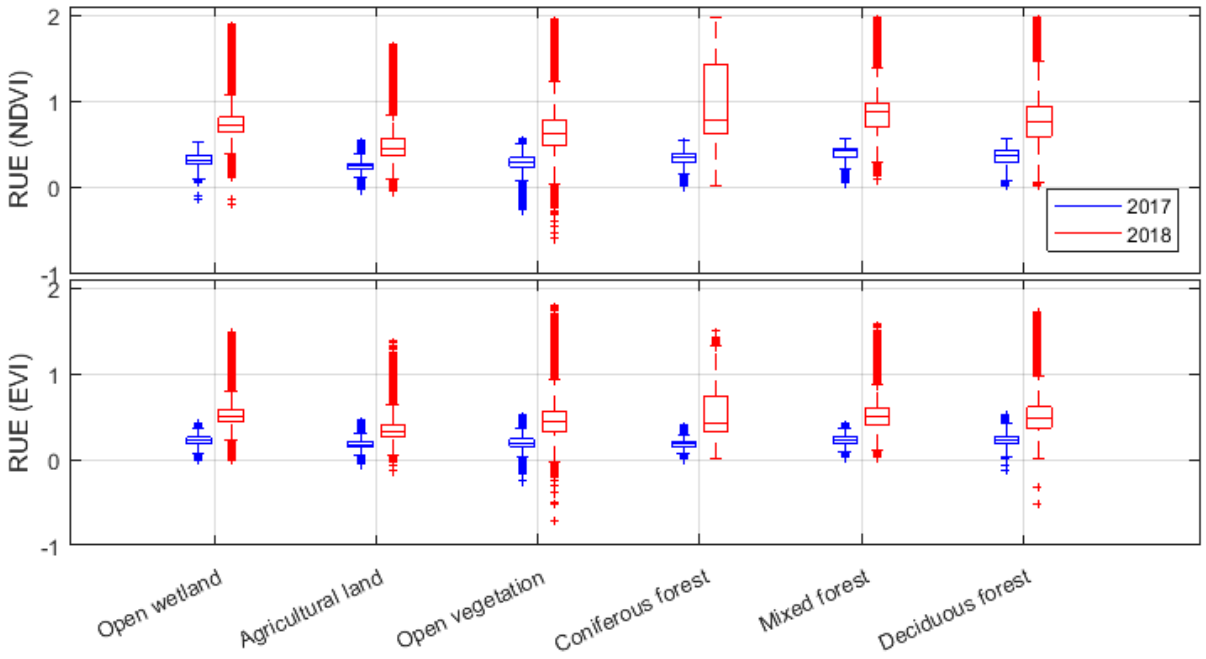

Figure 11. Boxplot showing the distribution of RUE_{NDVI} and RUE_{EVI} for each land cover class during the growing seasons in 2017 and 2018. The box shows the 25th to the 75th percentile, and the line in the box represents the median. The whiskers include values up to +/-2.7σ.

The median RUE_{NDVI} and RUE_{EVI} values for all land covers have increased, but there is also a larger span of values in 2018 than in 2017 (Figure 11). The largest relative increase in median for both RUE_{NDVI} and RUE_{EVI} is seen coniferous forest by followed by wetland and open vegetation. The smallest change in both relative and actual values is found in agricultural land (Table 8 and Appendix B, Table B8). Table 9 shows the relative changes in standard deviation between 2017 and 2018, and the SD has increased significantly for all land covers. The largest differences are seen in forested areas and the smallest are seen in agricultural land and wetlands.

Table 8. The relative change in median RUE_{NDVI} and RUE_{EVI} for each land cover type between 2017 and 2018. All changes are statistically significant using a two sample Wilcoxon signed rank test at a 0.05 level. Values for each year and actual changes can be found Appendix B (Table B7 & B8).

	Open wetland	Agricultural land	Open vegetation	Coniferous forest	Mixed forest	Deciduous forest
Δ RUE_{NDVI}	1,280	0,897	1,236	1,285	1,159	1,065
Δ RUE_{EVI}	1,318	0,895	1,263	1,358	1,187	1,106

Table 9. Relative change in standard deviation of RUE_{NDVI} and RUE_{EVI} for each land cover type between 2017 and 2018. All changes are statistically significant using a two sample Ansari-Bradley test at a 0.05 level. Values for each year and actual changes can be found Appendix B (Table B9 & B10).

	Open wetland	Agricultural land	Open vegetation	Coniferous forest	Mixed forest	Deciduous forest
Δ RUE_{NDVI}	2,307	1,825	2,745	4,914	3,918	3,242
Δ RUE_{EVI}	1,823	1,624	2,387	4,347	3,373	2,938

4.2.3. By crop

There are larger differences in growing patterns over the season between crops than between land cover types (Figure 12). The VI values for cereal crops seem to have an increasing slope in the beginning of the season and a decreasing slope at the end of the season. Barley has lower initial VI values, with a sharper increase between the first and second image both years, compared to wheat. The VI values for the cereal crops are quite similar for both years during the first, second and fourth date, but have lower values in the third image of 2018. For rapeseed, the largest difference is also seen in the third images of each year. Other crops like sugar beets, and vegetables have an increasing trend throughout the season. Sugar beets and vegetables both have similar VI patterns. As opposed to the cereal crops and rapeseed, the largest decrease between 2017 and 2018 is not during the third date, but during the fourth. The values for the first and second image are quite similar between the years for both sugar beets and vegetables. But the VI values are higher for vegetables in 2018 than in 2017 during the third image. It is also interesting to note, that there is a difference between how different indices respond; there is a decrease in the NDVI and EVI values for third image for the cereal crops and rapeseed in 2018 compared to 2017, but this decrease is smaller in NDWI.

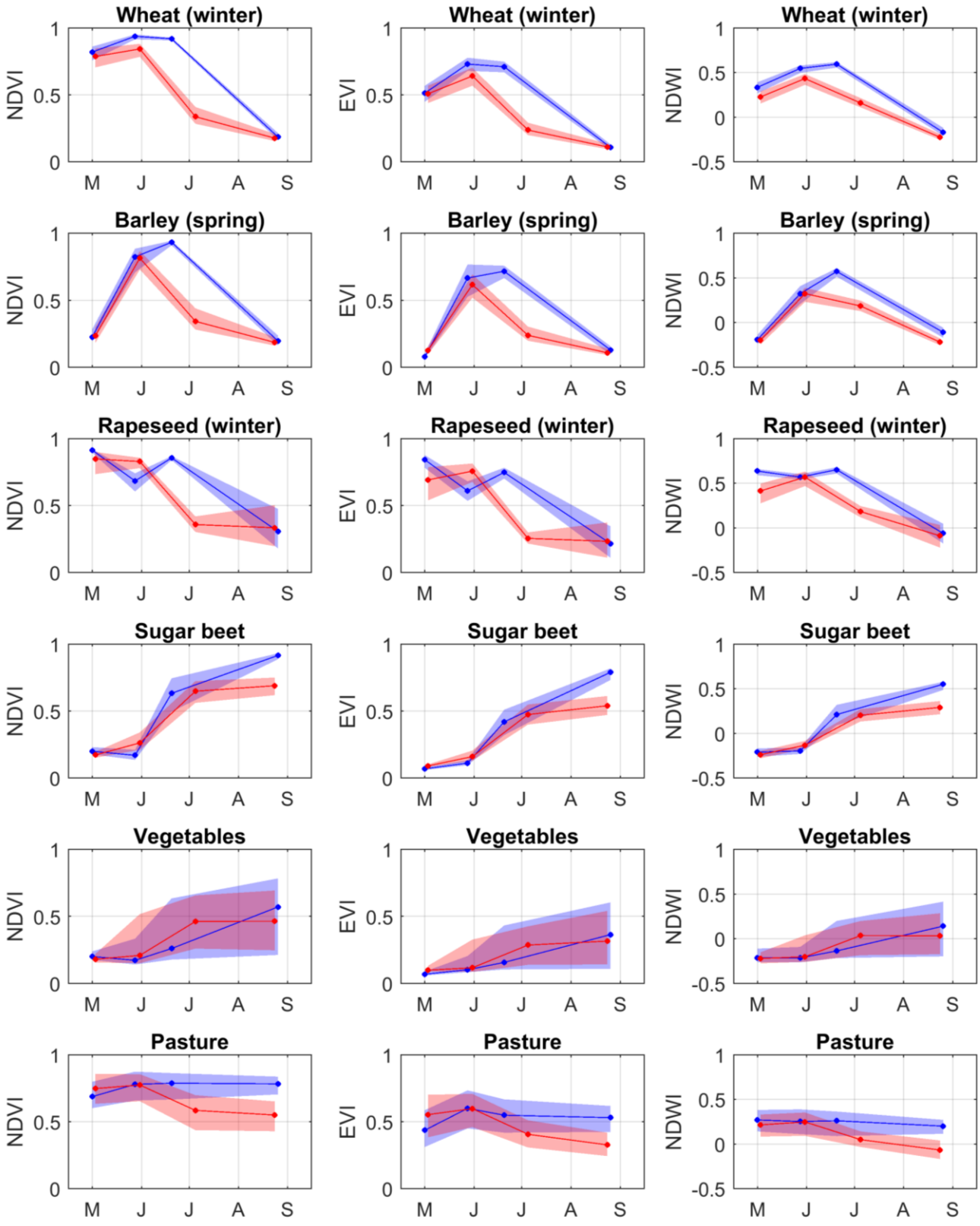

Figure 12. The medians of each image for each crop type presented as lines, and the 25th-75th percentiles presented as shaded areas of the NDVI, EVI and NDWI during the growing season for the study area for 2017(blue) and 2018 (red)

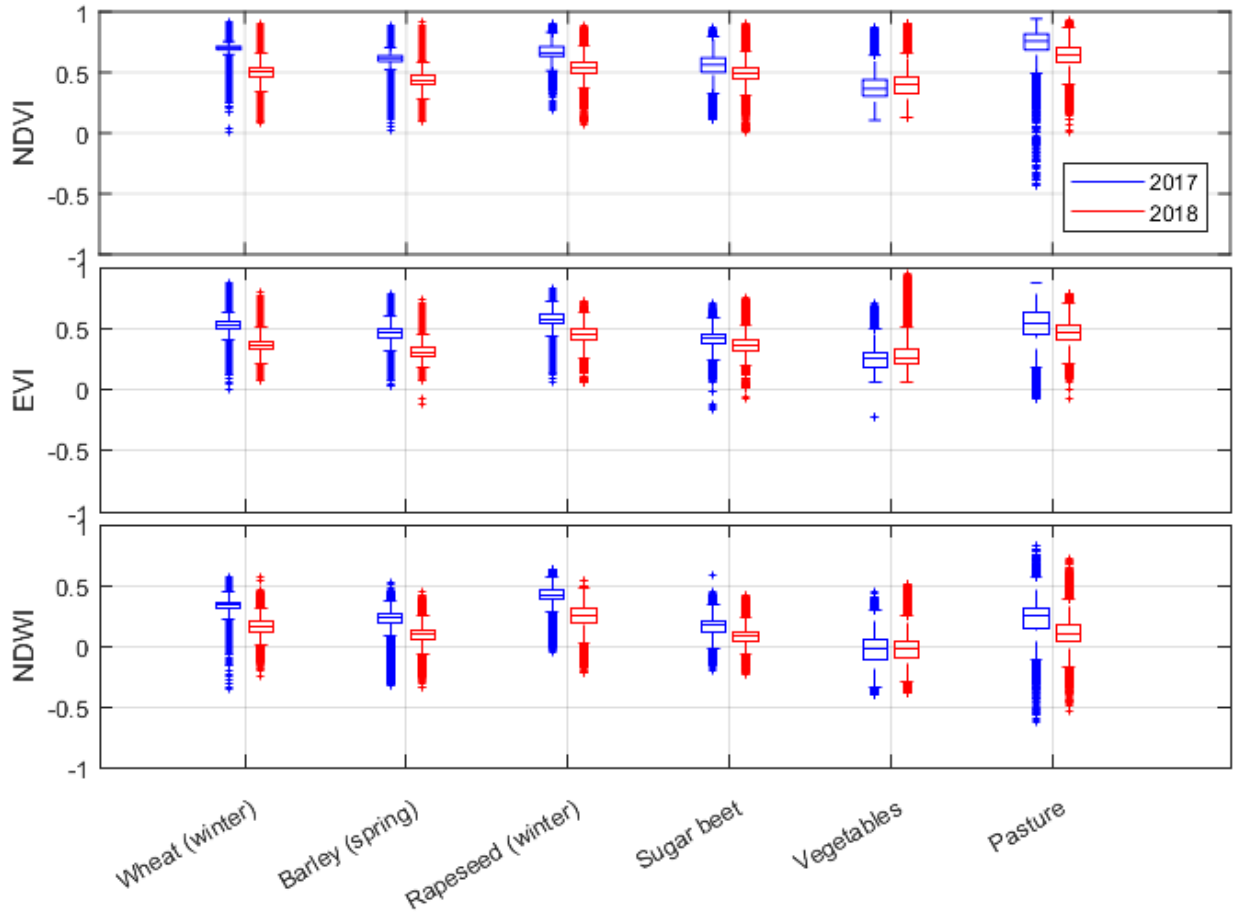

Figure 13. Boxplot showing the distribution of seasonal means of NDVI, EVI and NDWI for each crop type during the growing seasons in 2017 and 2018. The box shows the 25th to the 75th percentile, and the line in the box represents the median. The whiskers include values up to +/-2.7σ.

The distribution VI's for the crop types can be seen in Figure 13. Once again it can be seen that the values are generally lower in 2018 than in 2017, apart from for vegetables which have higher values for NDVI and EVI. Table 10, displays the changes in median VI values for the crops between 2017 and 2018. The largest decreases are seen in wheat, barley and rapeseed for all VI's except NDWI, where larger decreases can be seen in pasture. Interestingly, the only crop type that has any increasing VI values between the years is vegetables, where there is an increase in NDVI and EVI. However, the water content index NDWI have lower values but this change is not statistically significant.

*Table 10. Relative change in median NDVI, EVI and NDWI for each crop type between 2017 and 2018. The **bold** values are **not** statistically significant using a two sample Wilcoxon signed rank test at a 0.05 level. Negative changes are shaded. Values for each year and actual changes can be found Appendix B (Table B11 & B12).*

	Wheat (winter)	Barley (spring)	Rapeseed (winter)	Sugar beet	Vegetables	Pasture
Δ NDVI	-0,290	-0,306	-0,178	-0,119	0,078	-0,157
Δ EVI	-0,312	-0,350	-0,221	-0,140	0,035	-0,141
Δ NDWI	-0,528	-0,635	-0,400	-0,548	**-0,172**	-0,667

Table 11. Relative change in standard deviation of NDVI, EVI and NDWI for each crop type between 2017 and 2018. All changes are statistically significant using a two sample Ansari-Bradley test at a 0.05 level. Negative changes are shaded. Values for each year and actual changes can be found Appendix B (Table B13 & B14).

	Wheat (winter)	Barley (spring)	Rapeseed (winter)	Sugar beet	Vegetables	Pasture
Δ NDVI	0,890	0,288	0,228	-0,125	-0,092	-0,081
Δ EVI	0,169	-0,060	0,154	-0,136	0,019	-0,237
Δ NDWI	0,214	-0,044	0,463	-0,148	-0,096	-0,155

The changes in SD for the chosen crops and VI's between 2017 and 2018 can be seen in Table 11. The changes in SD show less clear patterns than the changes observed in medians in Table 10. For wheat and rapeseed there is an increase in SD. The increase is larger in NDVI and EVI for wheat, and in NDWI for rapeseed. For barley, there is a decrease in SD for all VI's except NDVI. For the other crops the SD has generally decreased, apart from in EVI for vegetables.

RUE has generally increased for all the crops (Figure 14) as it has for the whole study area. The smallest increases in median are seen in barley for both RUE_{NDVI} and RUE_{EVI}, followed by vegetables and larger increases are seen in sugar beets, and pastures (Table 12). Table 13 shows the difference in SD between 2018 and 2017. The largest increase in SD of RUE is seen in pasture and sugar beet, and the smallest increase is seen in rapeseed for RUE_{NDVI} and in barley for RUE_{EVI}.

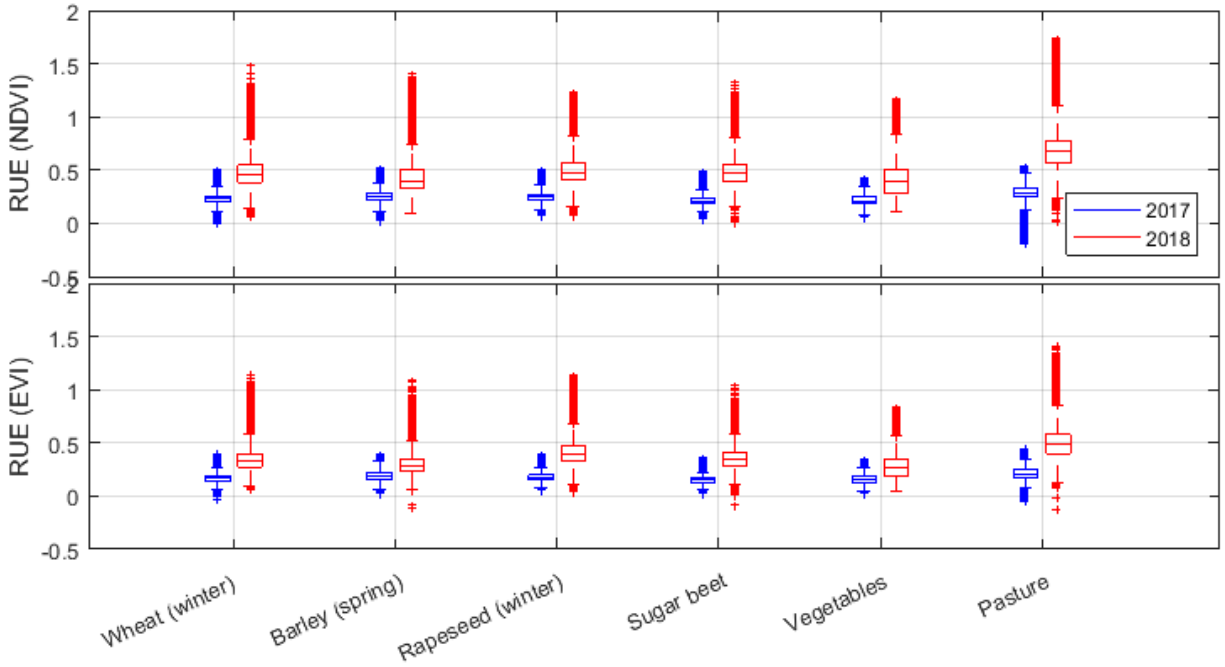

Figure 14. Boxplot showing the distribution of RUE_{NDVI} and RUE_{EVI} for each crop type during the growing seasons in 2017 and 2018. The box shows the 25th to the 75th percentile, and the line in the box represents the median. The whiskers include values up to +/-2.7σ.

Table 12. Relative change in median RUE_{NDVI} and RUE_{EVI} for each crop type between 2017 and 2018. All changes are statistically significant using a two sample Wilcoxon signed rank test at a 0.05 level. Values for each year and actual changes can be found Appendix B (Table B15 & B16).

	Wheat (winter)	Barley (spring)	Rapeseed (winter)	Sugar beet	Vegetables	Pasture
Δ RUE_{NDVI}	0,976	0,599	0,935	1,217	0,858	1,297
Δ RUE_{EVI}	0,970	0,488	1,177	1,278	0,693	1,319

Table 13. Relative change in standard deviation of RUE_{NDVI} and RUE_{EVI} for each crop type between 2017 and 2018. All changes are statistically significant using a two sample Ansari-Bradley test at a 0.05 level. Values for each year and actual changes can be found Appendix B (Table B17 & B18).

	Wheat (winter)	Barley (spring)	Rapeseed (winter)	Sugar beet	Vegetables	Pasture
Δ RUE_{NDVI}	2,269	1,721	1,663	2,916	1,723	2,951
Δ RUE_{EVI}	2,038	1,090	1,917	2,701	1,593	2,044

5. Discussion

5.1. Vegetation response

5.1.1. The whole study area

Based on the *in situ* data we could see that 2018 was an unusually warm and dry summer. Although some summers have been similarly dry, no other summer has had the combination of such high temperatures and such low precipitation since 1980.

The results show that the dry weather has most likely affected the vegetation, as the vegetation indices show lower values in 2018 for most of the area. There are some small patches where the VI's had higher values in 2018. However, comparing field by field would be misleading, as the increase in a VI in particular field might just be the result of a difference in crops farmed in that location between the two years. Although the decrease in VI values is probably largely attributed to the dry weather, other things could also have affected the results, such as the cold and wet spring of 2018. The majority of the study area is agricultural land, and the differences between the two years are most likely enhanced by differences between the cereal crops which are discussed further in section *5.1.3*.

The change in RUE for the whole area was positive, which could indicate that most of the vegetation has some resilience against lower precipitation. The large difference in RUE between the two years is likely a result of the unusually high precipitation in 2017 (see Figure 5). Similar results have been seen in previous studies; Ponce-Campos et al. (2013) found the lowest RUE values across different biomes during the wettest years. During high precipitation not all precipitation is available to the plant as some will disappear as runoff, recharging of groundwater, and an increased amount of precipitation is stored by the soil (Fensholt & Rasmussen, 2011; Ponce-Campos et al., 2013).

RUE is based on the assumption that there is a relationship between precipitation and vegetation productivity, as has been found in arid areas where precipitation is a limiting actor for vegetation growth (Higginbottom & Symeonakis, 2014). However, this relationship is not linear (Fensholt & Rasmussen, 2011; Higginbottom & Symeonakis, 2014), and often becomes weaker with higher precipitation as it is no longer a limiting factor for vegetation health (Ponce-Campos et al., 2013). Precipitation is normally not considered a limiting factor for vegetation in southern Sweden (Roerink et al., 2003), especially not during wet years such as 2017, which means that the assumption made might not have been correct. The fact that the relationship between vegetation and precipitation is likely very weak in the study area during these years, mean that changes in RUE most likely cannot be used as a measure of drought resilience, as the results are mostly a result of decreasing precipitation.

5.1.2. By land cover

The largest decrease in VI values between 2017 and 2018 was seen in agricultural land, and the smallest decreases were seen in the forest land cover types, especially coniferous and mixed forests. The lower VI values for agricultural land in the beginning of the season observed in 2018 could be due to the cold spring, and late sowing of both winter and spring crops in this season (Holmblad et

al., 2019) as a wet spring can make sowing more difficult (Wiréhn, 2018). However, only rapeseed and wheat had lower values for all VI's at the beginning of the season in 2018, and the differences in winter wheat were rather small. The lower values in the beginning of the season could also be due to a shift from winter crops towards spring crops as response to the late harvest in 2017. Both winter wheat and winter rapeseed decreased by 4% each in area between the years, whereas spring barley and sugar beets increased in area by 6% and 2% respectively. Regardless of what caused this difference and to what extent, it results in a difference even before the summer drought, which affect the results for the whole season.

This shift could also have affected the VI values for the whole area, as the majority of the area is used for agriculture. This points towards the importance of considering the difference in crops and areal distribution of crops between the years, when comparing land covers with a varied composition, either by taking the composition into account, or by breaking the agricultural land cover class down into smaller categories or individual crops with similar temporal growing patterns. The largest difference in agricultural land between the two years are seen in the third image, and similar to the decreases in values seen in wheat, barley and rapeseed seen at the same time. The results for individual crops and how they have affected the results for the whole area and the agricultural land cover class will be discussed in the next section.

In previous droughts it has been observed that the decreases in VI values for crop land and pastures are larger and have an earlier onset than the decreases in forest land covers (Zaitchik et al., 2006). Although, we do not have enough images to comment on the onset of the drought response, the decreases in VI values were larger in open vegetated areas than in the forest land covers. The decrease in seasonal VI seen in wetland between 2017 and 2018 were smaller than for agricultural land and open vegetation. It is possible that the higher initial water content meant that the decrease is a bit smaller.

The forest land cover classes generally had a smaller decrease in VI values than other land covers. These results are similar to the findings of Buras et al. (2019) and Zaitchik et al. (2006). Mixed forest had the smallest decrease and largest increases for all VI's. This suggests that the combination of coniferous and deciduous species are more drought resilient than the two forest types grown separately and in line with the findings of Gazol and Camarero (2016) and Pretzsch et al. (2013). In this study the land cover forest types were grouped together into the classes deciduous, coniferous, and mixed forest and it is therefore difficult to make further species-specific comparisons to literature.

In terms of changes in SD, there was a decrease in all non-forest land cover types, with the largest decrease in the agricultural land, followed by open vegetation. This is probably because drought conditions will make these land covers either get closer to the colour of bare soil, or become more uniformly brown. The changes in standard deviation for the forest land covers are generally positive, except for EVI for coniferous forest where a slight decrease can be seen. This could point to a larger patchiness of the forest areas, or an uneven response to drought.

RUE is significantly higher for all land covers in 2018 compared to 2017. The largest actual change in RUE us seen in mixed forest, but in terms of relative changes both wetland and open vegetation had larger increases in RUE than mixed forest. Agricultural land had the smallest actual and relative increase in RUE between 2017 and 2018 and is probably the least drought resilient land cover. Although this could indicate that agricultural land is the least drought resilient land cover and that mixed forest is not the most drought resilient land cover, the weak relationship between productivity and precipitation in this area, means that it is difficult to draw conclusions about drought resilience based on RUE.

5.1.3. By crop

It is clear from the results and previous studies (Wardlow et al., 2007) that different crops have different temporal growing patterns. In the results section we could see that winter wheat and rapeseed that were sown the autumn before had high VI values at the beginning of the season, but low at the end of the season; the spring barley which was planted in spring, had a similar pattern but had slightly lower VI values in the beginning of the season.

The largest decreases in VI values between 2017 and 2018 could be seen in the cereal crops (wheat and barley) and rapeseed for most VI's. These results seem to agree with Jordbruksverket (2018a) reporting yields 33% lower than usual for winter wheat and rapeseed, and 40% lower than usual for spring barley (Holmblad et al., 2019). In terms of actual changes between the two years wheat had the largest negative change, but in relative values the largest negative changes were seen in barley, in line with Holmblad et al. (2019).

Cereal crops commonly use escape strategies during heat and drought stress, which result in an earlier maturation of plants, and often a lower yield (Barnabás et al., 2008), both of which was reported in 2018 (Holmblad et al., 2019). This behaviour can make it difficult to measure drought of cereal crops with just a few satellite images per year, as it might be difficult to know what phenological state is being captured. It is likely that the last satellite image in late august is in fact just capturing bare soil in the areas where cereal crops and rapeseed is grown, but the differences in the VI values for these dates will still affect the overall result.

The difference in timing between the pictures means that we are missing out on crucial parts of the growing stages, and in this case the difference in cereals and rapeseed between 2017 and 2018 is enhanced. The third image in 2018 is likely capturing either partially harvested fields or maturing crops, whereas these three crops probably have not reached the same stage in the third image from 2017, as the VI values are still quite high at this point. The cereal crops 2017 reached maturity a bit later in the season (Holmblad et al., 2017), but this decrease in VI values which probably happened between the third and fourth image in 2017 (Wardlow et al., 2007) is not shown. The VI values for the cereal crops and rapeseed in 2018 are most likely still lower than 2017, but not as much lower as the results in this study suggest. Winter wheat, rapeseed and barley make up approximately 60 % of the agricultural land, and 40% of the whole study area. This means that the impact of the enhanced

difference due to lack of data is large both on the whole study area, and on the agricultural land cover class.

The VI values for sugar beets decreased less than the cereal crops and it was seen in the results that they have a different growing pattern compared to the cereal crops. They start growing a bit later in the season, but were planted unusually late both in 2017 and 2018 (Holmblad et al., 2019; Holmblad et al., 2017). This means that none of these years are normal for sugar beets. Sugar beets use avoidance and tolerance strategies as a response to drought, which include growing more roots as a response to drought (Romano et al., 2013). This could be one explanation to the smaller decrease in VI values for sugar beets between the two years. Although sugar beets are expected to gain from warmer and earlier springs in northern Europe, drought losses are still expected to increase, especially since breeding of sugar beets so far has not been focused on drought tolerance (Jones et al., 2003).

Vegetables was the only crop category with higher values in 2018 than in 2017 for EVI and NDVI, however the difference is relatively small compared to the other crops. Although higher values were seen in 2018, the reported yields were lower (Jordbruksverket, 2019b). The higher values for the growing season in 2018 are probably a result of higher values in July, but the values at the end of the season were lower in 2018, which could have affected the yield negatively. The category called vegetables contains many different plant species and types such as onion, carrots, salad and cabbage (Jordbruksverket, 2015) which makes it difficult to compare to other data and literature. We also do not know how the composition of vegetables and how it changed between the two years.

As opposed to the other crops mentioned above, pasture is not a farmed crop which is sown or harvested in the same way, and it therefore seems to have a bit more stable values over the season, especially in 2017. Decreases in yield (Smit et al., 2008) and VI values (Zaitchik et al., 2006) of grasslands and pasture have been observed in previous droughts such as in the drought in Europe 2003.

The SD has less clear patterns for crops than for other land covers. It could be that the responses are different for different crops, and the VI values for pasture becomes more uniformly low, whereas for rapeseed there could be an increased patchiness resulting in higher SD. There could also be a connection to whether the crops are winter or spring crops, as there was a decrease in SD for most VI's for sugar beets, vegetables, and barley which are all spring crops, whereas for rapeseed and wheat which are winter crops there was an increase in SD for most VI's between 2017 and 2018.

Both RUE and SD of RUE increased for all crop types between the years. Vegetables had the second lowest increase in RUE after barley even though vegetables had the largest positive change in VI's between the two years. This could mean that despite the larger increase in VI values in vegetables, vegetables might not be more drought resilient than wheat which had the second largest decrease in VI values between the two years. The largest increase in RUE was seen in pasture and sugar beets. However, as noted in previous sections, the RUE values should be interpreted with caution.

5.2. Differences between indices

NDVI and EVI are two of the most commonly used indices for measuring vegetation health and did generally show similar patterns for most land covers and crops in the results. However, NDVI generally had higher values than EVI and larger changes between the two years, and also showed larger differences between the two years in actual numbers. This could be due to NDVI reaching higher values and having a steeper increase in values than EVI as a response to the same change in vegetation (Jiang et al., 2008). As mentioned in the background, this is a trait that makes EVI more suitable for measuring differences in areas of high biomass, where NDVI has often reached its maximum value (Jiang et al., 2008) but in this study area the vegetation is not very dense; NDVI might therefore be more useful for spotting changes.

The changes in relative values have been larger for NDWI than for the other VI values, which could partially be explained by the fact that NDWI generally has lower values, and more values closer to zero than the other indices. However, NDWI did also have larger differences between the two years in actual numbers for some crops and landcovers.

There are also differences in the behaviour between the vegetation health/greenness indices (NDVI and EVI) and NDWI. For example, for the crop types wheat, barley and rapeseed in 2018, there is a sharp decrease between the second and third image in NDVI and EVI and then a very small change between the third and the fourth image. The fourth image of the season is most likely bare soil for these crops, in the third image in 2018 NDVI and EVI have similar values to the fourth. NDWI for these crops have a different pattern, with a smaller drop in values between the second and third image, and another drop in values between the third and fourth image. This could be interpreted as crops reaching maturation and therefore being drier and less green, resulting in lower NDVI and EVI, especially since NDVI can't distinguish between dry vegetation and bare soil (Delegido et al., 2015) but it might still not be as dry as bare soil, and therefore having a smaller decrease in water content index NDWI. An index such as the Green Brown Vegetation Index (GBVI) which can also measure dry vegetation, and distinguish between bare soil and vegetation (Delegido et al., 2015) could have given more information about the ground cover during the different dates.

5.3. Limitations and possible improvements

5.3.1. Data

There are some problems with this study out of which the timing of the Sentinel-2 data is the most important. The first, second and fourth images are taken on similar dates on both years, just a few days apart. However, the third image of each seasons are approximately two weeks apart. This is a long time, and means that there is a an almost two month gap between the third and fourth image in 2017. These dates were chosen as especially the summer of 2017 was very cloudy, but having more images for each year, at more similar dates between June and August would have given more information about the differences between the two years.

In section 5.1.3, it is discussed how the lack of images for each year cause an enhanced difference

between the two years. This would be resolved if data of much higher temporal resolution would have been used as this is needed to capture the different stages in the growing cycle of different crops. The selection of images was made based on completely could free images, however, it would have been possible to also use partially cloudy images, and mask out the cloudy areas to produce a time series with more dates, but less available pixels per date (Gómez-Chova et al., 2017). This approach might have filed in the gaps and given more information about how the values changed over the season.

There is also a problem with the difference in spatial and temporal resolution between datasets. All imagery used in this study has been resampled to 10 by 10-meter resolution for pixel by pixel analysis to be possible. However, the initial resolution of the gridded rainfall dataset is very coarse in comparison with to the other datasets. The coarse resolution creates very sharp boundaries between grid shaped areas of high precipitation and other grid shaped areas of low precipitation, whereas in reality precipitation gradients are often more continuous, although there can still be large spatial variations. It is impossible to know how the rainfall is distributed in each cell, and a possible source of error that needs to be considered for the calculations where it has been used together with datasets of higher spatial resolution, as it not only affects the results, but also the distribution and variation of values.

The possible dates of the satellite imagery are limited to the frequency of which the satellite is passing the study area, and the usefulness of the images is dependent on many different factors such as cloudiness, aerosols among others. Other datasets such as the gridded and *in situ* precipitation data sets, don't have the same date limitations, and are therefore using standardised timescales, such as precipitation per month. In this study it was assumed that the precipitation each month was uniform, although this is most likely not the case, and the precipitation of the full months were used in calculations. Future studies could gain from using data of higher and/or matching temporal resolution, to reduce the sources of error caused by differences in time scale.

The land cover data is based on classification of Sentinel-2 data from 2018 and lidar data. In classification of remote sensing data there is a risk of pixels being misclassified. Some pixels contain mixed land covers, and have been classified as one or the other, or a different land cover (Ahlkrona et al., 2018). This means that there could be a slight error in the results, especially in land covers that cover very small and disconnected areas, and in borders between land cover classes (Ahlkrona et al., 2018). The same land cover dataset was used for both years as it is assumed that there are no large changes between the years, however, there are still some changes, which mean that there could be an added error in the VI data for land cover data in 2017.

As mentioned in the method the crop data is based on crop census data (Jordbruksverket, 2018a). It is continuously verified with comparisons with aerial imagery, and in some cases when the data is difficult to verify based on images, Jordbruksverket are doing visits to check that the data provided is correct (Jordbruksverket, 2019a). The reliability is therefore very high. However, this data is originally in vector form and has been transformed into raster data of the same resolution as the other

datasets. This adds another source of error, especially at the edges of each field where mixed pixels might occur as a result of the transformation.

5.3.2. Methods

As discussed in the previous sections the current method with just four images taken each year is not suitable for comparing crops such as cereals which have a varying timing of maturity and very clear stages in the growing cycle during which it has different spectral properties (Wardlow et al., 2007). It works better for the land cover classes which tend to have more stable VI values over the season such as the forest land covers, or where there is a clear trend such as in sugar beets. In these cases even with fewer images, the deviations will more likely point to the effect of changed growing conditions for the plants.

For the time series visualisations in this study, it is assumed that the change between the dates is linear. This is not the case for most crops for crops like winter wheat, corn and sorghum (Wardlow et al., 2007). In previous studies it has been seen that the VI patterns for crops like wheat looks more like a curve with low values int the beginning and end of the growing cycle and higher values in the middle (Jonsson & Eklundh, 2002; Wardlow et al., 2007). With a larger number of images, fitting a curve to the points could therefore have given a better estimate of the VI values but also given more information about the growing season (Jonsson & Eklundh, 2002) and different stages of the growing cycle (Sakamoto et al., 2005),

In this study only two years are used; one dry year and one wet year. The wet year is representing a slightly more normal year, as the temperature is more normal. But adverse effects have been reported in 2017 as well, due to other reasons, such as the large amounts of precipitation, the cold spell in late spring and the unstable weather (Holmblad et al., 2017). By using data from more years with more available dates, reference data could be created with typical temporal curves for different crops, which could be compared to years of drought in order to see the impacts of drought during a year more clearly. In this study we can see how the years relate to each other, but not how the VI values of these years fit in the bigger picture. The choice of two consecutive years also means that they are not completely separate, as the vegetation in 2018 is affected by the precipitation (Reichmann et al., 2013) and crops (Jordbruksverket, 2018b) the year before.

6. Conclusion

The summer of 2018 stood out as one of the warmest and driest summers in the study area since 1980. The precipitation was almost 50% lower than the summer before. As a result there was a decrease in NDVI, EVI and NDWI and an increase in RUE_{NDVI} and RUE_{EVI} for most of the study area between the growing seasons in 2017 and 2018. It was found that the land cover with the least negative changes in VI values was mixed forest. Both coniferous and deciduous forest had more negative changes than mixed forest. This suggests that the combination of tree types might increase the drought resilience of mixed forests. However, the standard deviation of the forest classes also increased, pointing to a varied response to drought. The land cover with the largest decrease was agricultural land and it is likely the least drought resilient land cover in the study area. The break-down of the changes by crops showed that although the difference between the two years is likely attributed to drought, part of the decrease in VI values between the years in agricultural land could be explained by a shift from winter crops to spring crops due to the late harvest in 2017. It could also be a result of the satellite imagery from the different years being taken at different dates, and capturing different stages of the growing cycle which would affect the cereal crops and rapeseed in particular. The crop with the largest decrease in VI values was winter wheat and spring barley, pointing towards these crops being less drought resilient than sugar beet and vegetables which had smaller differences between 2017 and 2018.

Both RUE and the standard deviation of RUE increased for the whole study area between the two years. This could partially be due to the wet summer of 2017 causing very low RUE values that year and therefore enhancing the difference in RUE between 2017 and 2018. RUE was used in an attempt to measure drought resilience; the land cover class with the largest actual change in RUE was coniferous forest and mixed forest, but both wetland and open vegetation had a larger relative increase than mixed forest. For the crops the largest increase in RUE was seen in pasture and sugar beets, and not in vegetables which had largest increase in VI values. However, there is no strong relationship between precipitation and vegetation productivity in the study area, and these results should therefore be interpreted with caution.

The study has some weaknesses; the main one being the small number of satellite images for each year, which means that crucial information about the growing cycle is missing. There is also a difference in temporal and spatial resolution between the different data, which makes them more difficult to combine and which causes an error in RUE. The use of just two different years means that all results are relative to each other, and the differences could be a result of anomalous values either of these years.

The 2018 drought was shown to have a marked impact on the vegetation in the study area in Vellinge, Sweden. To better predict and prepare for future drought events, more research in the area would be beneficial. Future studies could gain from using more images for each year to better capture changes over the season, and using data for more than just two years in order to put the results into a historical perspective.

References

Aftonbladet. (2017a). Här föds skitvädret – som förstör sommaren. Retrieved 2019-07-02 from https://www.aftonbladet.se/nyheter/a/WVKW2/har-fods-skitvadret--som-forstor-sommaren

Aftonbladet. (2017b). Sämsta sommarvärmen – på 155 år. Retrieved 2019-07-02 from https://www.aftonbladet.se/nyheter/a/72q4w/samsta-sommarvarmen--pa-155-ar

AghaKouchak, A., Farahmand, A., Melton, F. S., Teixeira, J., Anderson, M. C., Wardlow, B. D., & Hain, C. R. (2015). Remote sensing of drought: Progress, challenges and opportunities. *Reviews of Geophysics, 53*(2), 452-480. doi:10.1002/2014rg000456

Ahlkrona, E., Cristvall, C., Jönsson, C., Mattisson, A., & Olsson, B. (2018). *Nationella marktäckedata basskikt*. Retrieved from

Alcamo, J., Moreno, J. M., Nováky, B., Bindi, M., Corobov, R., Devoy, R., Giannakopoulos, C., Martin, E., Olesen, J. E., & Shvidenko, A. (2007). Climate Change 2007: Impacts, Adaptation and Vulnerability: Contribution of Working Group II to the Fourth Assessment Report of the Intergovernmental Panel on Climate Change. *Europe*, 541-580.

Anderson, T. W., & Darling, D. A. (1954). A test of goodness of fit. *Journal of the American statistical Association, 49*(268), 765-769.

Ansari, A. R., & Bradley, R. A. (1960). Rank-sum tests for dispersions. *The Annals of Mathematical Statistics, 31*(4), 1174-1189.

Bai, Z. G., Dent, D. L., Olsson, L., & Schaepman, M. E. (2008). Proxy global assessment of land degradation. *Soil use management, 24*(3), 223-234.

Barnabás, B., Jäger, K., & Fehér, A. (2008). The effect of drought and heat stress on reproductive processes in cereals. *Plant, cell, environmental Research Letters, 31*(1), 11-38.

Bartels, D., & Souer, E. (2004). Molecular responses of higher plants to dehydration. In *Plant responses to abiotic stress* (pp. 9-38): Springer.

Boegh, E., Søgaard, H., Broge, N., Hasager, C., Jensen, N., Schelde, K., & Thomsen, A. (2002). Airborne multispectral data for quantifying leaf area index, nitrogen concentration, and photosynthetic efficiency in agriculture. *Remote Sensing of Environment, 81*(2-3), 179-193.

Bruce, W. B., Edmeades, G. O., & Barker, T. C. (2002). Molecular and physiological approaches to maize improvement for drought tolerance. *Journal of experimental botany, 53*(366), 13-25.

Buras, A., Rammig, A., & Zang, C. S. (2019). Quantifying impacts of the drought 2018 on European ecosystems in comparison to 2003. *arXiv preprint arXiv:1906.08605*.

Ceccato, P., Flasse, S., Tarantola, S., Jacquemoud, S., & Grégoire, J.-M. (2001). Detecting vegetation leaf water content using reflectance in the optical domain. *Remote Sensing of Environment, 77*(1), 22-33.

Chamaille-Jammes, S., Fritz, H., & Murindagomo, F. (2007). Spatial patterns of the NDVI–rainfall relationship at the seasonal and interannual time scales in an African savanna. *International Journal of Remote Sensing, 27*(23), 5185-5200. doi:10.1080/01431160600702392

Chaves, M. M., Maroco, J. P., & Pereira, J. S. (2003). Understanding plant responses to drought—from genes to the whole plant. *Functional plant biology, 30*(3), 239-264.

Ciais, P., Reichstein, M., Viovy, N., Granier, A., Ogee, J., Allard, V., Aubinet, M., Buchmann, N., Bernhofer, C., Carrara, A., Chevallier, F., De Noblet, N., Friend, A. D., Friedlingstein, P., Grunwald, T., Heinesch, B., Keronen, P., Knohl, A., Krinner, G., Loustau, D., Manca, G., Matteucci, G., Miglietta, F., Ourcival, J. M., Papale, D., Pilegaard, K., Rambal, S., Seufert, G., Soussana, J. F., Sanz, M. J., Schulze, E. D., Vesala, T., & Valentini, R. (2005). Europe-wide reduction in primary productivity caused by the heat and drought in 2003. *Nature, 437*(7058), 529-533.

Delegido, J., Verrelst, J., Rivera, J. P., Ruiz-Verdú, A., & Moreno, J. (2015). Brown and green LAI mapping through spectral indices. *International Journal of Applied Earth Observation Geoinformation, 35*, 350-358.

Du, L., Tian, Q., Yu, T., Meng, Q., Jancso, T., Udvardy, P., & Huang, Y. (2013). A comprehensive drought monitoring method integrating MODIS and TRMM data. *International Journal of Applied Earth Observation and Geoinformation, 23*, 245-253. doi:10.1016/j.jag.2012.09.010

Fensholt, R., & Rasmussen, K. (2011). Analysis of trends in the Sahelian 'rain-use efficiency' using GIMMS NDVI, RFE and GPCP rainfall data. *Remote Sensing of Environment, 115*(2), 438-451. doi:10.1016/j.rse.2010.09.014

Gao, B.-C. (1996). NDWI—A normalized difference water index for remote sensing of vegetation liquid water from space. *Remote Sensing of Environment, 58*(3), 257-266.

Gatti, A., Bertolini, A., Nasuti, C., & Carriero, F. (2015). Sentinel-2 products specification document. *ESA Standard Document*, 1 - 496.

Gazol, A., & Camarero, J. J. (2016). Functional diversity enhances silver fir growth resilience to an extreme drought. *Journal of Ecology, 104*(4), 1063-1075. doi:10.1111/1365-2745.12575

Glenn, E. P., Nagler, P. L., & Huete, A. R. (2010). Vegetation Index Methods for Estimating Evapotranspiration by Remote Sensing. *Surveys in Geophysics, 31*(6), 531-555. doi:10.1007/s10712-010-9102-2

Gómez-Chova, L., Amorós-López, J., Mateo-García, G., Muñoz-Marí, J., & Camps-Valls, G. (2017). Cloud masking and removal in remote sensing image time series. *Journal of Applied Remote Sensing, 11*(1), 015005.

Grasso, V. F., & Singh, A. (2011). Early warning systems: State-of-art analysis and future directions. *Draft report, UNEP, 1*.

Gu, Y., Brown, J. F., Verdin, J. P., & Wardlow, B. (2007). A five-year analysis of MODIS NDVI and NDWI for grassland drought assessment over the central Great Plains of the United States. *Geophysical Research Letters, 34*(6). doi:10.1029/2006gl029127

Hazaymeh, K., & Hassan, Q. K. (2017). A remote sensing-based agricultural drought indicator and its implementation over a semi-arid region, Jordan. *Journal of Arid Land, 9*(3), 319-330. doi:10.1007/s40333-017-0014-6

Higginbottom, T., & Symeonakis, E. (2014). Assessing land degradation and desertification using vegetation index data: Current frameworks and future directions. *Remote Sensing of Environment, 6*(10), 9552-9575.

Holmblad, J., Gerdtsson, A., Aldén, L., & Berg, G. (2019). *Växtskyddsåret 2018*. Retrieved from https://webbutiken.jordbruksverket.se/sv/artiklar/jo1814.html

Holmblad, J., Gerdtsson, A., Bölenius, E., Berg, G., Söderlind, C., & Benediktsson, A. (2017). *Växtskyddsåret 2017*. Retrieved from https://webbutiken.jordbruksverket.se/sv/artiklar/jo175.html

Huxman, T. E., Smith, M. D., Fay, P. A., Knapp, A. K., Shaw, M. R., Loik, M. E., Smith, S. D., Tissue, D. T., Zak, J. C., & Weltzin, J. F. (2004). Convergence across biomes to a common rain-use efficiency. *Nature, 429*(6992), 651.

Ji, L., Zhang, L., Wylie, B. K., & Rover, J. (2011). On the terminology of the spectral vegetation index (NIR − SWIR)/(NIR + SWIR). *International Journal of Remote Sensing, 32*(21), 6901-6909. doi:10.1080/01431161.2010.510811

Jiang, Z., Huete, A., Didan, K., & Miura, T. (2008). Development of a two-band enhanced vegetation index without a blue band. *Remote Sensing of Environment, 112*(10), 3833-3845. doi:10.1016/j.rse.2008.06.006

Jones, P., Lister, D., Jaggard, K., & Pidgeon, J. (2003). Future climate impact on the productivity of

sugar beet (Beta vulgaris L.) in Europe. *Climatic Change, 58*(1-2), 93-108.
Jonsson, P., & Eklundh, L. (2002). Seasonality extraction by function fitting to time-series of satellite sensor data. *IEEE transactions on Geoscience Remote Sensing of Environment, 40*(8), 1824-1832.
Jordbruksverket. (2015). Köksväxter. Retrieved 2019-07-10 from http://smakasverige.jordbruksverket.se/ravaror/informationsartiklar/artiklar/koksvaxter.504.html
Jordbruksverket. (2018a). Jordbruksverket. Retrieved 2019-02-20 from http://www.jordbruksverket.se/
Jordbruksverket. (2018b). Växtföljder i ekologisk odling. Retrieved 2019-07-25 from http://www.jordbruksverket.se/amnesomraden/miljoklimat/ekologiskproduktion/vaxtodling/ogras/vaxtfoljder.4.37cbf7b711fa9dda7a180001346.html
Jordbruksverket. (2019a). Fältgranskning av block. Retrieved 2019-07-29 from http://www.jordbruksverket.se/amnesomraden/tillsyn/faltgranskningavblock.4.3b6de5c115537b9383b446d2.html
Jordbruksverket. (2019b). Skörd av trädgårdsväxter 2018. Retrieved 2019-07-10 from http://www.jordbruksverket.se/webdav/files/SJV/Amnesomraden/Statistik,%20fakta/Tradgardsodling/JO37/JO37SM1901/JO37SM1901.pdf
Kadioglu, A., & Terzi, R. (2007). A dehydration avoidance mechanism: leaf rolling. *The Botanical Review, 73*(4), 290-302.
Kovats, R., Valentini, R., Bouwer, L., Georgopoulou, E., Jacob, D., Martin, E., Rounsevell, M., & Soussana, J. (2014). Climate change 2014: impacts, adaptation, and vulnerability. Part B: Regional aspects. *Europe*.
Larcher, W. (2000). Temperature stress and survival ability of Mediterranean sclerophyllous plants. *Plant biosystems, 134*(3), 279-295.
LeHouerou, H. N. (1984). Rain use efficiency: a unifying concept in arid-land ecology. *Journal of arid Environments*.
Li, B., Tao, S., & Dawson, R. W. (2002). Relations between AVHRR NDVI and ecoclimatic parameters in China. *International Journal of Remote Sensing, 23*(5), 989-999. doi:10.1080/014311602753474192
Li, Y., Ye, W., Wang, M., & Yan, X. (2009). Climate change and drought: a risk assessment of crop-yield impacts. *Climate research, 39*(1), 31-46.
Lichtenthaler, H. K. (1996). Vegetation Stress: an Introduction to the Stress Concept in Plants. *Journal of Plant Physiology, 148*(1-2), 4-14. doi:10.1016/s0176-1617(96)80287-2
LRF. (2018). 75 procent av böndernas inkomst torkade bort. Retrieved 2019-02-15 from https://www.lrf.se/mitt-lrf/nyheter/riks/2018/12/75-procent-av-bondernas-inkomst-torkade-bort/
Länsstyrelsen. (2018). Samlad information om torka och foderbrist i Skåne. Retrieved 2019-02-11 from https://www.lansstyrelsen.se/skane/om-lansstyrelsen-skane/nyheter-och-press/nyheter---skane/2018-07-25-samlad-information-om-torka-och-foderbrist-i-skane.html
Maracchi, G., Sirotenko, O., & Bindi, M. (2005). Impacts of present and future climate variability on agriculture and forestry in the temperate regions: Europe. *Climatic Change, 70*(1-2), 117-135.
Martínez-Ferri, E., Balaguer, L., Valladares, F., Chico, J., & Manrique, E. (2000). Energy dissipation in drought-avoiding and drought-tolerant tree species at midday during the Mediterranean summer. *Tree Physiology, 20*(2), 131-138.
Massey Jr, F. J. (1951). The Kolmogorov-Smirnov test for goodness of fit. *Journal of the American*

statistical Association, 46(253), 68-78.
McCrum-Gardner, E. (2008). Which is the correct statistical test to use? *British Journal of Oral Maxillofacial Surgery, 46*(1), 38-41.
Merlin, M., Perot, T., Perret, S., Korboulewsky, N., & Vallet, P. (2015). Effects of stand composition and tree size on resistance and resilience to drought in sessile oak and Scots pine. *Forest Ecology Management, 339*, 22-33.
Mittler, R. (2006). Abiotic stress, the field environment and stress combination. *Trends Plant Sci, 11*(1), 15-19. doi:10.1016/j.tplants.2005.11.002
Mondal, P. (2011). Quantifying surface gradients with a 2-band Enhanced Vegetation Index (EVI2). *Ecological Indicators, 11*(3), 918-924. doi:10.1016/j.ecolind.2010.10.006
Morin, X., Fahse, L., Scherer-Lorenzen, M., & Bugmann, H. (2011). Tree species richness promotes productivity in temperate forests through strong complementarity between species. *Ecology Letters, 14*(12), 1211-1219.
Nguyen, P., Shearer, E. J., Tran, H., Ombadi, M., Hayatbini, N., Palacios, T., Huynh, P., Braithwaite, D., Updegraff, G., Hsu, K., Kuligowski, B., Logan, W. S., & Sorooshian, S. (2019). The CHRS Data Portal, an easily accessible public repository for PERSIANN global satellite precipitation data. *Sci Data, 6*, 180296. doi:10.1038/sdata.2018.296
Nicholson, S., & Farrar, T. (1994). The influence of soil type on the relationships between NDVI, rainfall, and soil moisture in semiarid Botswana. I. NDVI response to rainfall. *Remote Sensing of Environment, 50*(2), 107-120.
Niemeyer, S. (2008). New drought indices. *Options Méditerranéennes. Série A: Séminaires Méditerranéens, 80*, 267-274.
Olesen, J. E., Børgesen, C. D., Elsgaard, L., Palosuo, T., Rötter, R., Skjelvåg, A., Peltonen-Sainio, P., Börjesson, T., Trnka, M., & Ewert, F. (2012). Changes in time of sowing, flowering and maturity of cereals in Europe under climate change. *Food Additives Contaminants: Part A, 29*(10), 1527-1542.
Olesen, J. E., Carter, T. R., Diaz-Ambrona, C., Fronzek, S., Heidmann, T., Hickler, T., Holt, T., Minguez, M. I., Morales, P., & Palutikof, J. P. (2007). Uncertainties in projected impacts of climate change on European agriculture and terrestrial ecosystems based on scenarios from regional climate models. *Climatic Change, 81*(1), 123-143.
Ponce-Campos, G. E., Moran, M. S., Huete, A., Zhang, Y., Bresloff, C., Huxman, T. E., Eamus, D., Bosch, D. D., Buda, A. R., & Gunter, S. A. (2013). Ecosystem resilience despite large-scale altered hydroclimatic conditions. *Nature Climate Change, 494*(7437), 349.
Pretzsch, H., Schütze, G., & Uhl, E. (2013). Resistance of European tree species to drought stress in mixed versus pure forests: evidence of stress release by inter-specific facilitation. *Plant Biology, 15*(3), 483-495.
Price, A. H., Cairns, J. E., Horton, P., Jones, H. G., & Griffiths, H. (2002). Linking drought-resistance mechanisms to drought avoidance in upland rice using a QTL approach: progress and new opportunities to integrate stomatal and mesophyll responses. *Journal of experimental botany, 53*(371), 989-1004.
Quarrie, S. A., Stojanović, J., & Pekić, S. (1999). Improving drought resistance in small-grained cereals: A case study, progress and prospects. *Plant Growth Regulation, 29*(1-2), 1-21.
Reichmann, L. G., Sala, O. E., & Peters, D. P. (2013). Precipitation legacies in desert grassland primary production occur through previous-year tiller density. *Ecology, 94*(2), 435-443.
Rhee, J., Im, J., & Carbone, G. J. (2010). Monitoring agricultural drought for arid and humid regions using multi-sensor remote sensing data. *Remote Sensing of Environment, 114*(12), 2875-2887. doi:10.1016/j.rse.2010.07.005

Rizhsky, L., Liang, H., Shuman, J., Shulaev, V., Davletova, S., & Mittler, R. (2004). When defense pathways collide. The response of Arabidopsis to a combination of drought and heat stress. *Plant physiology, 134*(4), 1683-1696.
Roerink, G. J., Menenti, M., Soepboer, W., & Su, Z. (2003). Assessment of climate impact on vegetation dynamics by using remote sensing. *Physics and Chemistry of the Earth, Parts A/B/C, 28*(1-3), 103-109.
Romano, A., Sorgona, A., Lupini, A., Araniti, F., Stevanato, P., Cacco, G., & Abenavoli, M. R. (2013). Morpho-physiological responses of sugar beet (Beta vulgaris L.) genotypes to drought stress. *Acta physiologiae plantarum, 35*(3), 853-865.
Rouse, J. W., Haas, R., Schell, J., & Deering, D. (1974). *Monitoring vegetation systems in the Great Plains with ERTS*. Paper presented at the NASA. Goddard Space Flight Center 3d ERTS-1 Symp.
Rouse, J. W., Haas, R. H., Schell, J., & Deering, D. (1973). *Monitoring the vernal advancement and retrogradation (green wave effect) of natural vegetation*. Retrieved from https://ntrs.nasa.gov/search.jsp?R=19730017588
Rötter, R. P., Höhn, J., Trnka, M., Fronzek, S., Carter, T. R., & Kahiluoto, H. (2013). Modelling shifts in agroclimate and crop cultivar response under climate change. *Ecology evolution, 3*(12), 4197-4214.
Sakamoto, T., Yokozawa, M., Toritani, H., Shibayama, M., Ishitsuka, N., & Ohno, H. (2005). A crop phenology detection method using time-series MODIS data. *Remote Sensing of Environment, 96*(3-4), 366-374.
Shao, H. B., Chu, L. Y., Jaleel, C. A., Manivannan, P., Panneerselvam, R., & Shao, M. A. (2009). Understanding water deficit stress-induced changes in the basic metabolism of higher plants - biotechnologically and sustainably improving agriculture and the ecoenvironment in arid regions of the globe. *Crit Rev Biotechnol, 29*(2), 131-151. doi:10.1080/07388550902869792
SMHI. (2016). Skånes klimat. Retrieved 2019-04-05 from https://www.smhi.se/kunskapsbanken/meteorologi/skanes-klimat-1.4827
SMHI. (2017). Sommaren 2017 - Typisk svensk sommar. Retrieved 2019-02-15 from https://www.smhi.se/klimat/klimatet-da-och-nu/arets-vader/sommaren-2017-meteorologi-1.123378
SMHI. (2019a). Ladda ner meteorologiska observationer - Nederbörd Falsterbo. Retrieved 2019-05-10 from https://www.smhi.se/data/meteorologi/ladda-ner-meteorologiska-observationer#param=precipitationMonthlySum,stations=all,stationid=52230
SMHI. (2019b). Ladda ner meteorologiska observationer - Temperatur Falsterbo. Retrieved 2019-05-10 from https://www.smhi.se/data/meteorologi/ladda-ner-meteorologiska-observationer#param=airTemperatureMeanMonth,stations=all,stationid=52230
Smit, H., Metzger, M., & Ewert, F. (2008). Spatial distribution of grassland productivity and land use in Europe. *Agricultural Systems, 98*(3), 208-219.
Spinoni, J., Vogt, J. V., Naumann, G., Barbosa, P., & Dosio, A. (2018). Will drought events become more frequent and severe in Europe? *International Journal of Climatology, 38*(4), 1718-1736.
Suhet. (2015). Sentinel-2 User Handbook, Issue 1, Rev 2, Revision 2. *ESA Standard Document*, 64.
Supit, I., Van Diepen, C., De Wit, A., Wolf, J., Kabat, P., Baruth, B., & Ludwig, F. (2012). Assessing climate change effects on European crop yields using the Crop Growth Monitoring System and a weather generator. *Agricultural Forest Meteorology, 164*, 96-111.
Toreti, A., Belward, A., Perez-Dominguez, I., Naumann, G., Luterbacher, J., Cronie, O., Seguini, L., Manfron, G., Lopez-Lozano, R., & Baruth, B. (2019). The exceptional 2018 European

water seesaw calls for action on adaptation. *Earth's Future*, *7*(6), 652-663.
Trnka, M., Olesen, J. E., Kersebaum, K. C., Skjelvåg, A. O., Eitzinger, J., Seguin, B., Peltonen-Sainio, P., Rötter, R., Iglesias, A., Orlandini, S., Dubrovský, M., Hlavinka, P., Balek, J., Eckersten, H., Cloppet, E., Calanca, P., Gobin, A., Vučetić, V., Nejedlik, P., Kumar, S., Lalic, B., Mestre, A., Rossi, F., Kozyra, J., Alexandrov, V., Semerádová, D., & Žalud, Z. (2011). Agroclimatic conditions in Europe under climate change. *Global Change Biology*, *17*(7), 2298-2318. doi:10.1111/j.1365-2486.2011.02396.x
Trnka, M., Rötter, R. P., Ruiz-Ramos, M., Kersebaum, K. C., Olesen, J. E., Žalud, Z., & Semenov, M. A. (2014). Adverse weather conditions for European wheat production will become more frequent with climate change. *Nature Climate Change*, *4*(7), 637.
Tucker, C. J., Vanpraet, C. L., Sharman, M., & Van Ittersum, G. (1985). Satellite remote sensing of total herbaceous biomass production in the Senegalese Sahel: 1980–1984. *Remote Sensing of Environment*, *17*(3), 233-249.
Turner, N. C. (1986). Crop water deficits: a decade of progress. In *Advances in agronomy* (Vol. 39, pp. 1-51): Elsevier.
Wardlow, B. D., Egbert, S. L., & Kastens, J. H. (2007). Analysis of time-series MODIS 250 m vegetation index data for crop classification in the US Central Great Plains. *Remote Sensing of Environment*, *108*(3), 290-310.
Varela, S. A., Gyenge, J. E., Fernandez, M. E., & Schlichter, T. J. T. (2010). Seedling drought stress susceptibility in two deciduous Nothofagus species of NW Patagonia. *24*(3), 443-453.
Wilcoxon, F., Katti, S., & Wilcox, R. A. (1970). Critical values and probability levels for the Wilcoxon rank sum test and the Wilcoxon signed rank test. *Selected tables in mathematical statistics*, *1*, 171-259.
Wiréhn, L. (2018). Nordic agriculture under climate change: A systematic review of challenges, opportunities and adaptation strategies for crop production. *Land Use Policy*, *77*, 63-74. doi:https://doi.org/10.1016/j.landusepol.2018.04.059
Zaitchik, B. F., Macalady, A. K., Bonneau, L. R., & Smith, R. B. (2006). Europe's 2003 heat wave: a satellite view of impacts and land–atmosphere feedbacks. *International Journal of Climatology: A Journal of the Royal Meteorological Society*, *26*(6), 743-769.
Zargar, A., Sadiq, R., Naser, B., & Khan, F. I. (2011). A review of drought indices. *Environmental Reviews*, *19*(NA), 333-349. doi:10.1139/a11-013
Zhao, Y., Wang, X., & Vázquez-Jiménez, R. (2018). Evaluating the performance of remote sensed rain-use efficiency as an indicator of ecosystem functioning in semi-arid ecosystems. *International Journal of Remote Sensing*, *39*(10), 3344-3362.
Åström, C., Bjelkmar, P., & Forsberg, B. (2019). High mortality during the 2018 heatwave in Sweden. *Lakartidningen*, *116*.

Appendices

Appendix A – All land covers and crops

This section shows all different land covers and crop types that were present in the study area during 2017 and 2018.

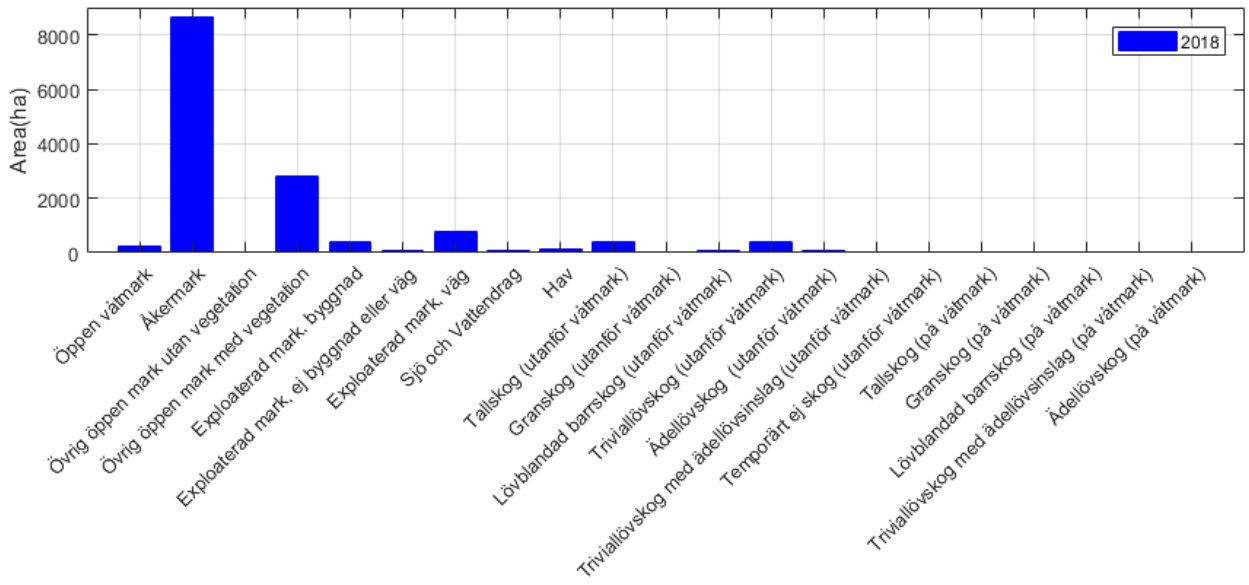

Figure A1. The distribution of land covertypes in the study area, based on land cover data from Naturvårdsverket (Ahlkrona, Cristvall, Jönsson, Mattisson, and Olsson, 2018)

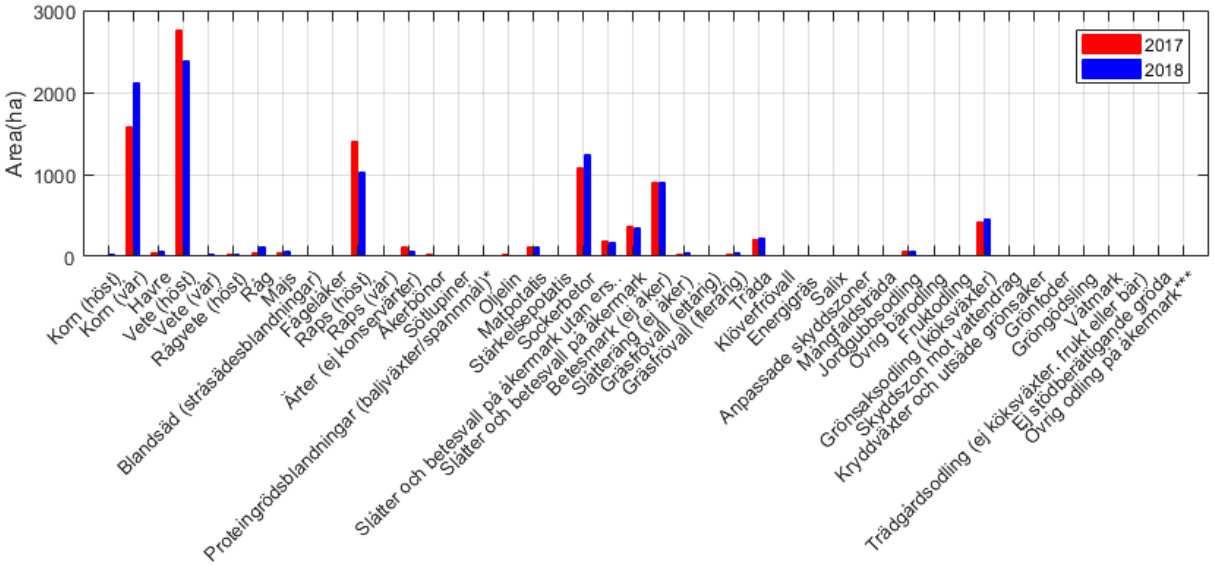

Figure A2. The crops farmed in the study area in hA in 2017 and 2018 based on the data from Jordbruksverket (2018a)

Appendix B – Vegetation Index and Rain use efficiency values

This section contains tables with vegetation index, precipitation and rain use efficiency values for 2017 and 2018, and the actual changes in values between the two years, for all landcover and crop type categories.

Table B1. Median and standard deviation in NDVI, EVI, NDWI, Precipitation, RUE_{NDVI} and RUE_{EVI} in 2017.

	NDVI		EVI		NDWI		Prec		RUE_{NDVI}		RUE_{EVI}	
	2017	**2018**	**2017**	**2018**	**2017**	**2018**	**2017**	**2018**	**2017**	**2018**	**2017**	**2018**
Median	0,663	0,509	0,478	0,360	0,246	0,114	305,0	150,0	0,248	0,497	0,175	0,351
SD	0,197	0,177	0,149	0,123	0,162	0,131	40,44	37,96	0,091	0,303	0,063	0,194

Table B2. Actual change in medians and standard deviation of NDVI, EVI, NDWI, Precipitation, RUE_{NDVI} and RUE_{EVI} for the whole study area. All differences are statistically significant, the change in median was tested with a two sample Wilcoxon signed rank test, and the change in SD was tested with a two sample Ansari-Bradley test. The negative changes are shaded.

	NDVI	EVI	NDWI	Prec	RUE_{NDVI}	RUE_{EVI}
Δ median	-0,154	-0,118	-0,132	-155,0	0,249	0,176
Δ SD	-0,020	-0,027	-0,030	-2,479	0,212	0,131

Table B3. Median NDVI, EVI and NDWI for each land cover type in 2017 and 2018.

	Open wetland		Agricultural land		Open vegetation		Coniferous forest		Mixed forest		Deciduous forest	
	2017	**2018**	**2017**	**2018**	**2017**	**2018**	**2017**	**2018**	**2017**	**2018**	**2017**	**2018**
NDVI	0,757	0,699	0,654	0,489	0,717	0,606	0,744	0,711	0,841	0,845	0,792	0,746
EVI	0,501	0,488	0,498	0,354	0,472	0,411	0,365	0,372	0,453	0,472	0,483	0,468
NDWI	0,249	0,167	0,282	0,118	0,198	0,088	0,219	0,202	0,306	0,302	0,255	0,200

*Table B4. Actual change in median NDVI, EVI and NDWI for each land cover type between 2017 and 2018. The **bold** values are **not** statistically significant at a 0.05 level using a two sample Wilcoxon signed rank test. The negative changes are shaded.*

	Open wetland	Agricultural land	Open vegetation	Coniferous forest	Mixed forest	Deciduous forest
Δ NDVI	-0,058	-0,165	-0,111	-0,033	**0,004**	-0,046
Δ EVI	-0,012	-0,144	-0,061	0,008	0,019	-0,016
Δ NDWI	-0,083	-0,164	-0,110	-0,017	-0,003	-0,055

Table B5. Standard deviation in NDVI, EVI and NDWI for each land cover type in 2017 and 2018.

	Open wetland		Agricultural land		Open vegetation		Coniferous forest		Mixed forest		Deciduous forest	
	2017	**2018**	**2017**	**2018**	**2017**	**2018**	**2017**	**2018**	**2017**	**2018**	**2017**	**2018**
NDVI	0,110	0,117	0,119	0,101	0,179	0,166	0,137	0,149	0,144	0,162	0,156	0,177
EVI	0,134	0,116	0,113	0,091	0,160	0,134	0,089	0,085	0,105	0,110	0,123	0,128
NDWI	0,129	0,134	0,141	0,102	0,138	0,124	0,103	0,109	0,123	0,131	0,120	0,128

Table B6. Actual change in standard deviation of NDVI, EVI and NDWI for each land cover type between 2017 and 2018. All changes are statistically significant at a 0.05 level using a two sample Ansari-Bradley test. The negative changes are shaded.

	Open wetland	Agricultural land	Open vegetation	Coniferous forest	Mixed forest	Deciduous forest
Δ NDVI	0,007	-0,018	-0,013	0,011	0,018	0,020
Δ EVI	-0,018	-0,022	-0,026	-0,003	0,005	0,005
Δ NDWI	0,005	-0,039	-0,015	0,006	0,008	0,008

Table B7. Median RUE_{NDVI} and RUE_{EVI} for each land cover type in 2017 and 2018.

	Open wetland		Agricultural land		Open vegetation		Coniferous forest		Mixed forest		Deciduous forest	
	2017	**2018**	**2017**	**2018**	**2017**	**2018**	**2017**	**2018**	**2017**	**2018**	**2017**	**2018**
RUE_{NDVI}	0,311	0,718	0,236	0,452	0,283	0,628	0,348	0,776	0,420	0,866	0,372	0,748
RUE_{EVI}	0,218	0,507	0,171	0,329	0,195	0,441	0,182	0,429	0,235	0,501	0,233	0,485

Table B8. Actual change in median RUE_{NDVI} and RUE_{EVI} for each land cover type between 2017 and 2018. All changes are statistically significant at a 0.05 level using a two sample Wilcoxon signed rank test.

	Open wetland	Agricultural land	Open vegetation	Coniferous forest	Mixed forest	Deciduous forest
Δ RUE_{NDVI}	0,407	0,215	0,345	0,428	0,446	0,376
Δ RUE_{EVI}	0,289	0,158	0,245	0,247	0,266	0,252

Table B9. Standard deviation of RUE_{NDVI} and RUE_{EVI} for each land cover type in 2017 and 2018.

	Open wetland		Agricultural land		Open vegetation		Coniferous forest		Mixed forest		Deciduous forest	
	2017	**2018**	**2017**	**2018**	**2017**	**2018**	**2017**	**2018**	**2017**	**2018**	**2017**	**2018**
RUE_{NDVI}	0,074	0,245	0,057	0,160	0,086	0,323	0,076	0,451	0,085	0,417	0,094	0,399
RUE_{EVI}	0,061	0,172	0,049	0,129	0,067	0,228	0,044	0,237	0,058	0,253	0,068	0,268

Table B10. Actual change in standard deviation of RUE_{NDVI} and RUE_{EVI} for each land cover type between 2017 and 2018. All changes are statistically significant at a 0.05 level using a two sample Ansari-Bradley test.

	Open wetland	Agricultural land	Open vegetation	Coniferous forest	Mixed forest	Deciduous forest
Δ RUE_{NDVI}	0,171	0,103	0,237	0,374	0,332	0,305
Δ RUE_{EVI}	0,111	0,080	0,161	0,193	0,195	0,200

Table B11. Median NDVI, EVI and NDWI for each crop type in 2017.

	Wheat (winter)		Barley (spring)		Rapeseed (winter)		Sugar beet		Vegetables		Pasture	
	2017	**2018**	**2017**	**2018**	**2017**	**2018**	**2017**	**2018**	**2017**	**2018**	**2017**	**2018**
NDVI	0,703	0,500	0,618	0,431	0,660	0,540	0,564	0,498	0,366	0,395	0,758	0,643
EVI	0,522	0,360	0,467	0,307	0,574	0,446	0,418	0,361	0,252	0,261	0,545	0,470
NDWI	0,335	0,161	0,231	0,091	0,419	0,252	0,169	0,080	-0,016	-0,020	0,247	0,101

*Table B12. Actual change in median NDVI, EVI and NDWI for each crop type between 2017 and 2018. The **bold** values are **not** statistically significant at a 0.05 level using a two sample Wilcoxon signed rank test. The negative changes are shaded.*

	Wheat (winter)	Barley (spring)	Rapeseed (winter)	Sugar beet	Vegetables	Pasture
Δ NDVI	-0,202	-0,187	-0,120	-0,066	0,029	-0,116
Δ EVI	-0,162	-0,160	-0,128	-0,057	0,009	-0,075
Δ NDWI	-0,174	-0,140	-0,167	-0,089	**-0,004**	-0,147

Table B13. Standard deviation of NDVI, EVI and NDWI for each crop type in 2017 and 2018.

	Wheat (winter)		Barley (spring)		Rapeseed (winter)		Sugar beet		Vegetables		Pasture	
	2017	**2018**	**2017**	**2018**	**2017**	**2018**	**2017**	**2018**	**2017**	**2018**	**2017**	**2018**
NDVI	0,036	0,069	0,054	0,070	0,059	0,072	0,086	0,075	0,130	0,118	0,104	0,096
EVI	0,051	0,060	0,061	0,057	0,063	0,073	0,072	0,062	0,113	0,115	0,128	0,098
NDWI	0,052	0,063	0,064	0,061	0,062	0,091	0,070	0,059	0,130	0,117	0,131	0,111

Table B14. Actual change in standard deviation of NDVI, EVI and NDWI for each crop type between 2017 and 2018. All changes are statistically significant at a 0.05 level using a two sample Ansari-Bradley test. The negative changes are shaded.

	Wheat (winter)	Barley (spring)	Rapeseed (winter)	Sugar beet	Vegetables	Pasture
Δ NDVI	0,032	0,016	0,013	-0,011	-0,012	-0,008
Δ EVI	0,009	-0,004	0,010	-0,010	0,002	-0,030
Δ NDWI	0,011	-0,003	0,029	-0,010	-0,013	-0,020

Table B15. Median of RUE_{NDVI} and RUE_{EVI} for each crop type in 2017 and 2018.

	Wheat (winter)		Barley (spring)		Rapeseed (winter)		Sugar beet		Vegetables		Pasture	
	2017	**2018**	**2017**	**2018**	**2017**	**2018**	**2017**	**2018**	**2017**	**2018**	**2017**	**2018**
RUE_{NDVI}	0,229	0,451	0,250	0,399	0,246	0,478	0,211	0,468	0,211	0,395	0,290	0,672
RUE_{EVI}	0,165	0,325	0,189	0,282	0,176	0,388	0,149	0,341	0,153	0,261	0,209	0,491

Table B16. Actual change in median RUE_{NDVI} and RUE_{EVI} for each crop type between 2017 and 2018. All changes are statistically significant at a 0.05 level using a two sample Wilcoxon signed rank test.

	Wheat (winter)	Barley (spring)	Rapeseed (winter)	Sugar beet	Vegetables	Pasture
Δ RUE_{NDVI}	0,222	0,149	0,232	0,257	0,183	0,382
Δ RUE_{EVI}	0,160	0,093	0,212	0,192	0,108	0,282

Table B17. Standard deviation of RUE_{NDVI} and RUE_{EVI} for each crop type in 2017 and 2018.

	Wheat (winter)		Barley (spring)		Rapeseed (winter)		Sugar beet		Vegetables		Pasture	
	2017	**2018**	**2017**	**2018**	**2017**	**2018**	**2017**	**2018**	**2017**	**2018**	**2017**	**2018**
RUE_{NDVI}	0,049	0,159	0,048	0,130	0,045	0,120	0,039	0,153	0,057	0,156	0,060	0,235
RUE_{EVI}	0,041	0,123	0,046	0,097	0,037	0,108	0,031	0,115	0,050	0,130	0,052	0,159

Table B18. Actual change in standard deviation of RUE_{NDVI} and RUE_{EVI} for each crop type between 2017 and 2018. All changes are statistically significant at a 0.05 level using a two sample Ansari-Bradley test.

	Wheat (winter)	Barley (spring)	Rapeseed (winter)	Sugar beet	Vegetables	Pasture
Δ RUE_{NDVI}	0,110	0,082	0,075	0,114	0,098	0,176
Δ RUE_{EVI}	0,083	0,051	0,071	0,084	0,080	0,106